J. Membrane Biol. 179, 185–204 (2001)
DOI: 10.1007/s002320010047

The Journal of
Membrane
Biology

© Springer-Verlag New York Inc. 2001

Role of Pre-epithelial "Unstirred" Layers in Absorption of Nutrients from the Human Jejunum

J.R. Pappenheimer
Concord Field Station, Department of Biology, Harvard University, Old Causeway Road, Bedford, MA 01730, USA

Received: 5 September 2000/Revised: 31 October 2000

Abstract. Pre-epithelial "unstirred" layers (abbr. pL) are generally regarded as undesirable diffusion barriers that impede access to absorptive cells of exogenous hexoses, amino acids or other experimental probes added to fluids bathing the mucosal surface. In the present paper it is suggested that the pL may have a functional role. Diffusion plus convection of saccharides and oligopeptides from lumen to brush border, combined with absorption to blood of their hydrolytic products, confers rectifying properties to the pL. The proposed model, based on experimental data from segmental jejunal perfusions in normal human subjects, indicates that the functional pathway for diffusion plus convection through the pL of hexoses and amino acids bound in the form of oligomers is only 10 ± 2 μm or little more than the anatomical thickness of the glycocalyx and mucus layers. In contrast, the pathlength from brush border to lumenal perfusion fluid for diffusion minus convection of monomers generated by membrane bound hydrolases is 50–150 μm. According to this model the pL offers little resistance to the passage of saccharides or oligopeptides from lumen to brush border but at the same time it provides a protective blanket that diminishes diffusional losses to lumenal chyme of hexoses and amino acids generated in the brush border. The model provides a theoretical explanation for the "kinetic advantage" of transporting hexoses or amino acids through the pL in the form of oligomers and it predicts the proximal-distal concentrations of free glucose or fructose found experimentally in the outflows from jejunal segments perfused with sucrose or maltose.

Correspondence to: J.R. Pappenheimer, 63 Chilton St., Cambridge, MA 02138-6801, USA

Key words: Unstirred layers — Intestinal absorption — Paracellular solvent drag — Membrane hydrolysis

Introduction

The absorptive surfaces of the brush border are overlayed with the glycocalyx and a film of mucus 5–10 μm in thickness [61]. Overlying the mucus is an aqueous layer of chyme that is subject to variable degrees of mixing with the major contents of the intestinal lumen. Collectively the pre-epithelial layers are usually described as "unstirred layers" but this may be a misnomer not only because of variable mechanical mixing of lumenal contents by contractile elements in villi, muscularis mucosa and outer wall, but also because convective flow of fluid continually penetrates the layers and alters diffusion gradients. As stated by Gruzdkov et al. [25], ". . . the diffusion zone adjacent to the enterocyte apical membrane cannot be regarded as some immobile water layer. The transport of substances across this zone . . . is determined not only by its diffusion characteristics but also by the direction and intensity of the net transepithelial water flow."

Previous treatments of this topic have characterized the pL as an impediment to the transfer of free hexoses and amino acids from the intestinal lumen to the apical surface of absorptive cells. Although this interpretation of "unstirred layers" is applicable to experiments in which exogenous hexoses or amino acids are perfused through intestinal segments or otherwise presented to the mucosal surface, it is not directly relevant to normal physiological conditions. Normal products of lumenal digestion of carbohydrates, proteins or polypeptides are intermediate saccharides and peptides containing two to ten or more monomeric units [1]. Hexoses and amino acids therefore traverse the pL in the form of these in-

termediate products of digestion, rather than as free monomers. Final hydrolysis to free hexoses or amino acids occurs in the microenvironment of the brush border, catalyzed by membrane-bound hydrolyases of the microvilli [6, 58, 65, 67]. Theoretically, there is a kinetic advantage to the diffusive transport of hexoses or amino acids across the pL if they are transported in the form of polymers. The potential kinetic advantage derives from two factors (i) hydrolysis in the brush border followed by absorption of the monomeric products to circulating blood results in relatively high concentration gradients for diffusional flux of saccharides through the pL as shown in Fig. 5 below, and (ii) the number of monomers carried in a polymer is proportional to molecular weight (MW) of the polymer, whereas diffusional flux of the polymer is inversely proportional to $(MW)^{0.5}$. For any given molar concentration difference across the pL the diffusional flux of monomers arriving at the apical surface would therefore be expected to increase in proportion to the square root of the molecular weights of the parent polymers.

In Part I of the present paper evidence is presented that the functional pathway for diffusion plus convection of disaccharides through the pL is only 8–12 μm or little more than the anatomical thickness of the glycocalyx and mucus layers separating lumenal fluid from the apical surface of absorptive cells. In Part II the functional pathlength for diffusional back-flux to lumen of monomers formed in the brush border is estimated to be 50–150 μm. The pre-epithelial layers may therefore act functionally as a rectifier with a high conductance to flow of nutrients from lumen to the sites for final hydrolysis and transepithelial transport while at the same time acting as a protective blanket to minimize diffusional losses of the free hexoses and amino acids generated by membrane-bound hydrolases in the brush border of absorptive cells. This possibility was first pointed out by Gruzdkov [26] and I am indebted to him for providing me with a translation of his paper. The present discussion will focus mainly on experimental results obtained by many investigators from perfusions of jejunal segments in normal humans under conditions in which steady-state rates of absorption of saccharides, peptides and their hydrolysis products can be measured together with rates of fluid absorption.

Part I

Diffusive and Convective Transport of Disaccharides from Lumen to Brush Border of Perfused Jejunal Segments: Evaluation of Pathlength for Diffusion + Convection

Smithson, Millar, Jacobs and Gray [61] were the first to propose that hydrolysis rates of saccharides or peptides might be used to evaluate the thickness (∂) of "unstirred layers" overlying the epithelium of the small intestine. Their proposal was based on the following equation,

$$\partial = DA(K'_m - K_m)/0.5V'_{xh} \quad (1)$$

where D = diffusion coefficient of solute in pre-epithelial layers; A = surface area of fluid layers overlying the absorptive epithelium; V'_{xh} = maximum rate of hydrolysis in the segment, estimated by extrapolation of data relating flux to lumenal concentration; K'_m = mean concentration of the solute in the segment when hydrolysis rate is 50% of estimated V'_{max}; K_m = kinetic constant of enzyme-substrate reaction (Michaelis-Menten Constant) measured in vitro with enzymes purified from intestinal epithelium. A formal derivation of Eq. 1 is given in Appendix A of the present paper.

Smithson et al. applied Eq. 1 to hydrolysis rates of sucrose, lactose, and a tetrapeptide in perfused jejunal segments of anesthetized rats. Values of ∂ calculated from Eq. 1 for all three solutes were more than 600 μm, values which were (in the words of the authors) ". . . too large to be compatible with the known dimensions of the rat intestine." The undistended rat jejunum is in the form of a rectangular tube or flattened ellipse in which the central axis is everywhere within about 200 μm of the absorptive epithelium. To account for their anomalous results, Smithson et al. postulated that the diffusion coefficients of these small solutes through the mucus (unstirred) layers must be far less than in pure water. No direct measurements of diffusion through intestinal mucus are available but it seems unlikely that mucus-glycocalyx layers consisting mostly of water and having an anatomical thickness of less than 10 μm could restrict diffusion of small uncharged solutes by the two orders of magnitude necessary to explain the anomalous results. The glycocalyx overlying endothelial cells offers little or no restriction to diffusion of solutes of molecular weights less than 10,000 [45]. Smithson et al. did not include in their paper the essential data relating flux to lumenal concentrations and so there was no assurance that there is a true maximum to absorption of the test solutes as required by Eq. 1. Subsequent experiments by Gisolfi et al. [20], Levitt et al. [39] and analysis of older experiments by Holdworth & Dawson [29], Gray and Inglefinger [22], McMichael et al. [44], Sandle et al. [57] and others show that there is in fact no true maximum to absorption of sugars in perfused segments of human jejunum; instead, the absorptive fluxes of maltose, sucrose or glucose continue to increase almost linearly as lumenal concentrations are increased up to 100–200 mM as shown in Fig. 1. The absorption rates summarized in Fig. 1 are "physiological" in the sense that they were obtained with perfusion loads of CHO up to 200 mmols hr^{-1} or the caloric equivalent of about twice the normal metabolic rate of a 70 kg human (100 kC hr^{-1}). When

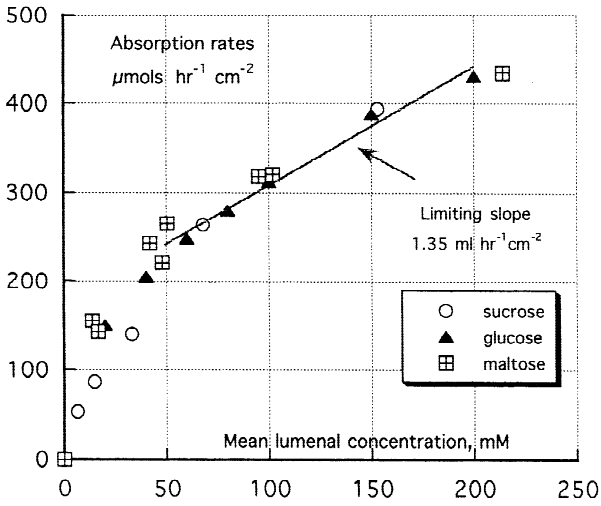

Fig. 1. Absorption rates of glucose, sucrose and maltose from perfused jejunal segments of normal humans. The glucose data are from Table 2, Col. B and represent the best fit to values published in references [15, 17, 18, 19, 20, 22, 29, 41, 64]. Values are calculated for lumenal surface area of 6.4 cm^2 per cm length of catheter. The standard deviation from a smooth curve drawn through all the glucose data is ±22% of the mean values. The sucrose data are from reference [22] and the maltose data are from references [23, 32, 44, 57]. In the 15–30 cm sampling lengths of catheters used for these perfusions the absorption rates of disaccharides and their hydrolysis products were always less than their rates of disappearance from the perfusion fluid (Col. B of Table 1) because some of the hydrolytic products generated in the brush border diffuse back to the lumenal perfusion fluid as explained in the text. The limiting slope of 1.35 ml hr^{-1} cm^{-2} in the concentration range 50–200 mM is directly proportional to net rate of fluid absorption and provides an estimate of $(1 - \sigma)\phi$ in Eq. 4 as explained in the text. At higher concentrations, fluid absorption is diminished by the osmotic pressure and becomes negative at concentrations exceeding 300 mM as shown in Fig. 3. This results in a diminished rate of increase of absorption of sugars that has been interpreted by some investigators as an approach to a transcellular transport maximum [22, 29, 43, 44].

plotted as mols t^{-1} cm^{-2} as in Fig. 1 it is evident that in the concentration range 50–200 mM all three sugars are cleared from perfusion fluids at approximately the same rates with a common limiting slope of about 1.3 ml hr^{-1} cm^{-2}. This previously unrecognized relationship has implications for understanding mechanisms of intestinal absorption as discussed below.

To explain the linear increase of absorption rates at high lumenal concentrations Levitt et al. [39] postulated that after saturation of maltases in upper regions of the villi, the excess unhydrolyzed maltose diffuses through interstices between villi where it is hydrolyzed and absorbed at depths up to 300 μm below the villous tips. This hypothesis is inconsistent with the fact that at high concentrations (60–200 mM) sucrose or exogenous glucose are cleared from jejunal perfusions at approximately the same rate as maltose (Fig. 1) despite large differences in their diffusion coefficients or rates of hydrolysis. It is also inconsistent with the fact that hydrolytic enzymes [67], glucose transporters [34], fluid absorption [37] and associated sodium concentrations [28, 60] are located near the villous tips. An alternative hypothesis is presented below.

Equation 1 and the models proposed by Smithson et al. [61] and by Levitt et al. [39] do not take account of the following two transport processes which alter interpretation of their results, both qualitatively and quantitatively.

Convective Transport Through the Pre-epithelial Layers

The hydrolysis of saccharides or peptides is normally associated with net fluid absorption powered by osmotic gradients generated by concentrative, carrier-mediated transepithelial transport of hydrolysis products (e.g., glucose, amino acids). This results in fluid flow through the pre-epithelial layers with associated convective transport of solutes. For example, normal 300 g rats provided with 5% glucose, maltose or egg albumen will drink and absorb 20 ml hr^{-1} steadily throughout their nocturnal feeding period: the absorbed fluid is excreted in urine at an average rate of about 15 ml hr^{-1} [49]. Exercising dogs [11] or humans [47] will drink and absorb large quantities of sugar solutions for many hours and the rates of fluid absorption per unit area of mucosal surface are almost ten times greater in humans than in rats [51]. Fluid absorption (convective flow) adds to diffusive transport in the direction lumen to brush border and at the same time reduces the diffusive losses of hydrolysis products in the direction brush border to lumen. Conversely, the secretion of fluid into the lumen retards diffusion through the pL. Under physiological conditions (but not during segmental perfusions) the periodic discharge of large osmotic loads from the stomach to the duodenum after a meal may result in initial secretion of fluid into the duodenum but normally net fluid absorption occurs throughout the length of the jejunum [4, 16]. Abnormal net fluid secretion into the jejunum may be induced by a variety of pathogens or drugs or during experimental perfusions with hypertonic solutions; under such abnormal conditions the convective component of solute fluxes through the pL becomes negative. The convective component is omitted entirely from Eq. 1.

Convective Transport of Unhydrolyzed Saccharides or Peptides from Brush Border to Blood Via Paracellular Solvent Drag

Equation 1 is based on the assumption that all of the saccharides or peptides lost from the perfusion fluid are hydrolyzed so that rates of hydrolysis can be equated with measured fluxes through the pre-epithelial layers; this is equivalent to assuming that none of the saccharides or peptides are absorbed into blood intact. It is

known, however, that significant quantities of ingested lipid-insoluble solutes in the molecular weight range 100–1000$^+$ Daltons are absorbed and can be recovered intact in urine, especially during high rates of fluid absorption. Thus, 50–80% of ingested creatinine (MW 113), dicyclopropylglycine (MW 155) or L-glucose (MW 180) and 50% of certain undegradable D-octapeptides (MW 780–850) are absorbed and excreted intact in urine of normal mice, rats, birds or humans [2, 33, 38, 49, 50]. Significant quantities of carbohydrate polymers as large as inulin (MW 5500) or Dextrans (MW 4400 to 17,200) can be absorbed paracellularly from perfused segments of jejunum in anesthetized rats [40, 48, 58]. It may therefore be expected that sucrose or maltose in concentrations high enough to saturate hydrolases in the villous tips will be absorbed to blood intact by paracellular convective flow; significant quantities of ingested maltose have in fact been detected in portal blood [36].

The following model of hydrolysis and absorption of saccharides is based on the principles embodied in Eq. 1 modified to include the additional transport processes described in paragraphs (i) and (ii) above. The new model accurately describes results obtained from perfused jejunal segments of human subjects by Gray & Ingelfinger [21], McMichael et al. [44], Jones, Higgins & Silk [32] and others.

The New Model and Its Applications

Proposition 1

During perfusion of jejunal segments the lumenal concentrations of disaccharides decrease exponentially along the length (l) of the intestine. The concentration at any distance (l) is then given by $C_l/C_i = e^{-kl}$ where $k = (\ln C_i/C_o)/l_o$ and subscripts i and o refer to measured values at inflow and outflow. Experimental evidence in support of this proposition for the case of sucrose is shown in Fig. 2. The mean concentration in the lumenal perfusion fluid (C_L) is then defined by

$$C_L = (C_i - C_o)/\ln(C_i/C_o) \quad (2)$$

For short segments under most experimental conditions the exponential mean is not significantly different from the linear average.

Proposition 2

At any point along the length of the perfused segment, the saccharides that reach the brush border are hydrolyzed at a rate defined by the Michaelis-Menten equation for first order enzyme reactions. When expressed as *mean* values along the length of the segment

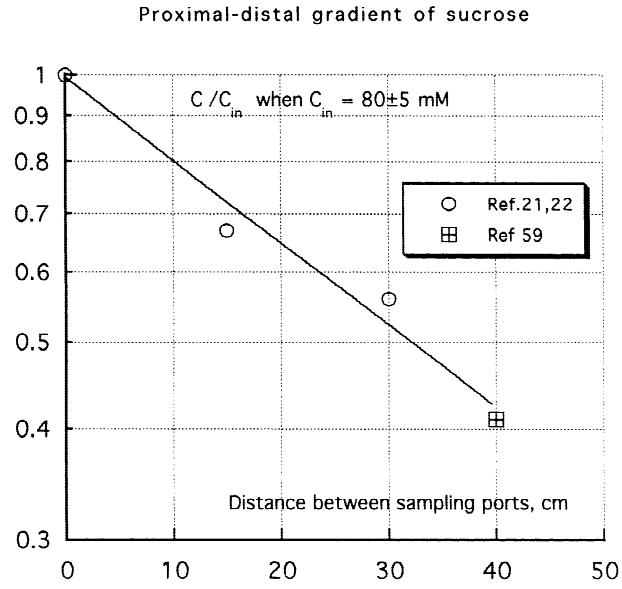

Fig. 2. Proximal-distal gradient of sucrose. There have been no systematic investigations to test the proposition that lumenal concentrations of disaccharides decrease exponentially with distance in perfused segments of the small intestine. The data shown for sucrose in Fig. 2 were obtained incidentally by Gray & Ingelfinger [21, 22] and by Shi et al. [59].

$$J_h = (V_{xh}C_b)/(C_b + K_m) \quad (3)$$

where J_h = mean rate of hydrolysis in the segment, mols t^{-1}; V_{xh} = maximum rate of hydrolysis after hydrolases are fully saturated with substrate; C_b = mean concentration of saccharide in the brush border; K_m = Michaelis-Menten affinity constant measured in vitro = 3 ± 1 mM for maltose and 18 ± 1 mM for sucrose [1, 24]. This proposition is the same as that underlying Eq. 1 utilized by Smithson et al. [61] and by Levitt et al. [39]; it is an approximation because of the nonlinear decrease of concentrations with distance.

Proposition 3

Unhydrolyzed saccharides in the brush border are entrained in paracellular fluid absorption and absorbed to blood at a rate defined by $(1 - \sigma)\phi J_v C_b$ where J_v = measured rate of fluid absorption: C_b = mean concentration of intact disaccharide in the brush border: ϕ = fraction of net fluid absorption that occurs paracellularly and σ = osmotic reflection coefficient at intercellular junctions.

Proposition 4

The steady-state flux of saccharide (J_S) through the preepithelial layers (i.e., its measured rate of disappearance from the perfusion fluid) is defined by

$$J_S = J_h + (1 - \sigma)\phi J_v C_b \quad (4)$$

It should be emphasized that the second term of Eq. 4 represents the component of total flux that is absorbed paracellularly in unhydrolyzed form. This component has been neglected in previous treatments but it becomes a significant contributor to total flux during absorption of large CHO loads as shown in Fig. 1. Substitution of Eq. 3 in Eq. 4 and solving for V_{xh}

$$V_{xh} = \{J_S - (1 - \sigma)\phi J_v C_b\}(C_b + K_m)/C_b \quad (5)$$

C_b in Eqs. 4 and 5 can be evaluated as a function of mean lumenal concentration by the following fundamental equation for diffusion in the presence of convection

$$J_S = J_v\{C_L e^{(J_v\partial/D)} - C_b\}/\{e^{(J_v\partial/D)} - 1\} \quad (6)$$

whence

$$C_b = C_L e^{(J_v\partial/D)} = J_S/J_v\{e^{(J_v\partial/D)} - 1\} \quad (7)$$

where J_S = measured rate of loss of saccharide from perfusion fluid per unit area, mols t^{-1} cm^{-2}; J_v = net fluid absorption per unit area or velocity, cm t^{-1}; C_L = mean concentration or saccharide in lumen = $(C_{in} - C_{out})/ln\ (C_{in}/C_{out})$; ∂ = pathlength for diffusion plus convection; D = diffusion coefficient.

Various forms of Eqs. 6 and 7 have been employed by previous investigators [3, 7, 10, 25, 54] to describe diffusion in the presence of convection in biological systems; a formal derivation is attached in Appendix B. The dimensionless number $J_v\partial/D$ is sometimes referred to as the Peclet number [7, 52, 54]. When $J_v\partial/D$ is less than about 0.2, $e^{J_v\partial/D} \approx 1 + J_v\partial/D$ (within 2%) and Eq. 6 reduces to the familiar form

$$J_s = (D/\partial)\,(C_L - C_b) + J_v C_L \quad (6a)$$

flux = diffusion + convection

It should be emphasized that previous models of absorption have neglected the paracellular component of flux (i.e., the linear component at high concentrations shown in Fig. 1) and have therefore overestimated the value of V_{xh} as determined by Eq. 5. Five of the terms in the six equations, namely J_S, J_v,C_l, D and K_m can be determined experimentally. The remaining three terms, namely C_b, V_{xh} and ∂ are unknowns but two of them, namely V_{xh} and ∂, are constants that are (theoretically) independent of lumenal concentrations. To solve for V_{xh} and ∂ it is only necessary to find the unique (constant) value of ∂ that leads to a constant value for V_{xh} that is independent of lumenal concentration.

Application of the Model to Estimate V_{xh} and ∂ in Human Jejunum

Diffusion Coefficients

The following calculations employ the free aqueous diffusion coefficients of glucose, sucrose or maltose measured at 25°C and corrected to 37°C [30]. For larger saccharides it is assumed that their free diffusion coefficients vary inversely with the square roots of their molecular weights as shown in Table 6. If the diffusion coefficients of sugars through pre-epithelial layers are less than in water, then the calculated values of ∂ represent virtual or "equivalent" pathlengths that will be *greater* than the true pathlength in proportion to the restriction to diffusion.

Intestinal Dimensions

Fluxes measured during perfusions of human intestinal segments are usually expressed per cm length, it being assumed implicitly that the length of intestine undergoing exchange of fluid or solutes is equal to the distance between sampling ports on the perfusion catheters. This assumption appears to be far from correct. The length of the relaxed, uncoiled small intestine measured at autopsy is about 600 cm in adult humans [62] and 700 cm in 60 kg gorillas [8], whereas the distance traveled by catheter tip from duodenum to ileo-cecal valve in normal, fasting adult humans is less than 300 cm [4, 16, 22]. This large discrepancy could be explained if the catheters bypass mucosal folds that are present in living, tonically contracting, coiled intestines but are absent in the uncoiled and relaxed (dead) intestines: whatever the reasons, it appears that the distance between sampling ports of a catheter may be very much less than the length of intestinal mucosa actually exposed to the perfusion fluid. Although the functional length of perfused segments may be indeterminate it is nevertheless possible to estimate the area of smooth lumenal surface per cm of catheter length from the distribution volume of dyes added to the perfusion fluid. Thus the volume of human jejunum perfused at the rate of 15 ml/min is 325 ± 65 ml per 100 cm of catheter length, as found by the dye dilution technique of Dillard, Eastman & Fordtran [12]. The surface area of a circular cylinder of equivalent volume is 6.4 ± 1.3 cm^2/cm and it will be assumed that this is the area of pL (per cm catheter length) available for exchange of fluid and solutes during perfusions of the human jejunum.

Fluid Exchange

Since absorption of solutes includes convective as well as diffusive flux (Eqs. 4 and 6) it is necessary to specify

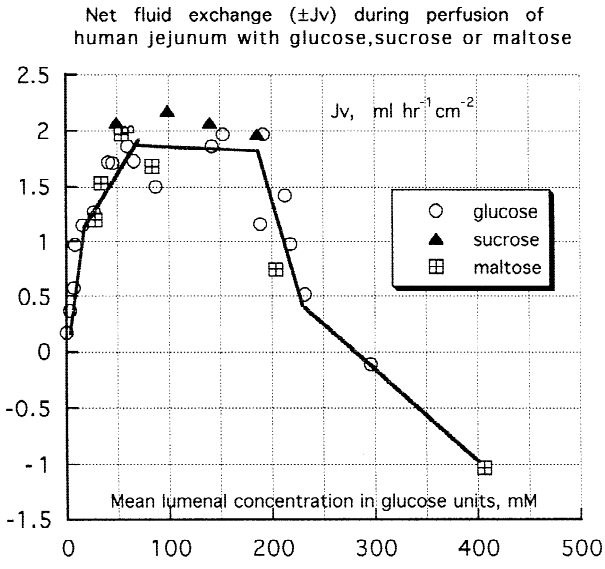

Fig. 3. Net fluid exchange during perfusion of human jejunum with glucose, sucrose or maltose. Mean lumenal concentrations are calculated from Eq. 2 and J_v is normalized to surface area as in Fig. 1. Data for glucose are from references [17, 18, 20, 29, 57], for sucrose from [20] and for maltose from [44, 57]. When concentrations are expressed in glucose units all three sugars induce approximately the same rates of fluid exchange, thus supporting the theory that fluid absorption is powered by transepithelial osmotic gradients associated with transport of glucose. The decrease in net fluid absorption at concentrations exceeding 200 mM decreases the paracellular solvent drag component of absorption of sugar and this is sometimes misinterpreted as an approach to a transcellular transfer maximum [22, 29, 43, 44].

net fluid absorption rates (J_v). Figure 3 summarizes rates of net fluid absorption during segmental perfusions of human jejunum with maltose, sucrose or glucose. Some publications relating absorption rates of hexoses or saccharides to lumenal concentrations do not include the data needed for calculating rates of fluid absorption. To include the flux data from these publications I assume that the rates of fluid absorption were equal to the average rates shown in Fig. 3. Inspection of Fig. 3 shows that at glucose concentrations in the range 60–180 mM the net absorption rate of fluid (J_v) is approximately constant (1.85 ± 0.2 ml hr^{-1} cm^{-2}). In this range, also, hydrolases are almost saturated and rates of hydrolysis (J_h) are constant. Under these conditions the absorptive fluxes are linearly related to concentration as predicted from Eq. 4 and shown in Fig. 1. The limiting linear slope $(1 - \sigma)\phi J_v = 1.35$ ml hr^{-1} cm^{-2} whence $(1 - \sigma)\phi = 1.35/1.85 = 0.7$. It is noteworthy that the fluid exchange rates per unit area and concentration of glucose units shown in Fig. 3 ($\pm J_v$) are approximately the same for maltose, sucrose and exogenous glucose. This, previously unrecognized, property of the small intestine supports the hypothesis that fluid absorption induced by carbohydrates is powered by osmotic gradients across tight junctions generated by Na-coupled, concentrative transport of the free glucose.

The parameters given in paragraphs 1–3 above, combined with observed values for fluxes, provide the data needed to solve Eqs. 4–7 for C_b, V_{xh} and ∂ at any given lumenal concentration and perfusion rate. The essential data are shown in Cols. A–E of Table 1. The corresponding calculated values of C_b, ∂ and V_{xh} shown in Cols. F and G are obtained as follows: an arbitrary value for ∂ is assumed and the corresponding values for C_b and V_{xh} for each inflow concentration are calculated from Eqs. 7 and 5, respectively. For the case of human jejunum perfused with sucrose an assumed pathlength (∂) of 10 μm resulted in a constant value for maximum rate of hydrolysis ($V_{xh} = 252 \pm 0$ μmols hr^{-1} cm^{-2}) as shown in Col. G. Similar calculations for a range of assumed pathlengths are plotted in Fig. 4; values of ∂ greater than about 15 μm lead to unacceptably large variations of calculated V_{xh} as a function of concentration. If our model is correct, a pathlength of 20 μm would be too long to permit sufficient flux of sucrose to account for observed rates of hydrolysis. Similarly, a pathlength of about 10 μm yields minimum SD for maximum hydrolysis rates of maltose in perfused segments of human jejunum. A pathlength as short as 8 μm could also fit the observed sucrose fluxes (within their experimental errors) but would be too short to fit the maltose data. These derived values for ∂ (10 ± 2 μm) are only 2–3× greater than the observed anatomical thickness of the mucus layer overlying the brush border of the jejunum (4.3 ± 1 μm, Ref [61]), thus indicating that the fibrous glycocalyx and the long-chain mucin molecules do not greatly restrict passage of small uncharged solutes. It is therefore unnecessary to postulate that diffusion of small solutes through pre-epithelial layers is greatly restricted as suggested by Smithson et al. [61] or that unhydrolyzed saccharides diffuse 300 μm into the clefts between villi before being hydrolyzed and absorbed as monomers as proposed by Levitt et al. [39].

When expressed per unit area of mucosal surface the maximum rate of hydrolysis of sucrose (i.e., 252 μmols hr^{-1} cm^{-2}) is approximately the same as that of maltose (Table 1). Reference to the experimental data of Fig. 1 indicates that absorption rates of sucrose or maltose exceed their maximal rates of hydrolysis at lumenal concentrations above 75 mM: at these concentrations the unhydrolyzed disaccharides are presumably absorbed intact by paracellular solvent drag in accordance with the second term of Eq. 4. For further analysis of the system it is useful to define the brush border concentrations (C_b) as a function of lumenal concentrations (C_l). Figure 5 shows this relationship for maltose and sucrose and for exogenous free glucose as determined in columns B and F of Table 1 and Columns A and E of Table 2. It is seen that the molar concentration gradients available for the

Table 1. Maximum rates of hydrolysis (V_{xh}) and pathlength (∂) for diffusion + convection of sucrose (A) or maltose (B) through pre-epithelial layers of perfused jejunal segments

A. Sucrose						
Segment length = 15 cm		Area = 96 cm^2	K_m = 18 mM	Q_i = 900 ml hr^{-1}		
A	B	C	D	E	F	G
C_i	C_L	J_S, [Ref] mmols/hr/seg. ± SD	selected J_S, within ± SD μmol/hr/sq. cm	J_v.ml/hr per sq. cm.	C_b (Eq. 7) for ∂ = 10 mμ	V_{xh}
10	6.2	5.7 ± 1.1, [22]	49	0.5	4.2	252
20	14.8	9.4 ± 2, [22]	100	0.7	10.8	252
40	31	15.7 ± 3.4, [22]	169	1.3	25.2	252
80	68	29.5 ± 8, [22]	260	1.6	61.2	252
160	153	43 ± 19, [22]	412	1.9	147.5	252
					Mean	252
					±SD	0
B. Maltose						
Segment length = 20–30 cm		Area = 128–192 cm^2	K_m = 3.3 mM	Q_i = 900–1200ml hr^{-1}		
10	4.3	8.6 ± 2*, [63]	72	0.4	1.2	266
28	14	25 ± 4, [57]	174	1.5	5.7	265
35	16.7	33 ± 13, [44]	193	1.5	7.6	266
40	20.5	28 ± 7*, [63]	215	1.6	10.6	266
70	42	63 ± 17, [44]	281	1.9	31.0	265
70	50.5	53 ± 14, [31]	298	1.9	39.4	266
80	48	58 ± 19, [23]	293	1.9	36.9	266
80	50	42 ± 10*, [63]	297	1.9	38.9	266
139	102	90 ± 25, [44]	346	1.4	91.0	266
					Mean	266
					±SD	0

C = concentration [subscripts *i*, inflow; *L*, mean lumenal; *b*, mean in brush border (Eq. 7)]; J = flux [subscripts *v*, net fluid; *s*, disaccharide]; ∂ = functional pathlength for diffusion + convection through pL, μm; V_{xh} = maximum rate of hydrolysis in perfused segment, μmols hr^{-1} cm^{-2}; Q_i = perfusion inflow, ml hr^{-1}.
* No data for *SD*, assume ± 25% of mean

diffusion of maltose are more than double those for exogenous glucose, thus providing a theoretical basis for explaining the "kinetic advantage" originally described by Crane [6, 42] and discussed in more detail in Part II below.

Transport of Exogenous Glucose Through Pre-epithelial Layers: Evaluation of K_{mg} and V_{xg} for the Carrier-Mediated, Transcellular Component of Glucose Absorption

In the preceding section the equivalent pathlength (∂) for diffusion + convection of solutes from lumenal fluid to brush border was evaluated from absorption and hydrolysis rates of maltose or sucrose. The calculated value was 10 ± 2 μm. Given this value for ∂, Eq. 7 predicts the brush border concentration (C_b) of any absorbable solute in terms of the measured quantities C_L, D, J_S, J_v and A. Application to the case of exogenous glucose perfused through jejunal segments of humans is shown in Table 2. There have been many investigations of glucose transport and fluid absorption in perfused jejunal segments of normal human subjects and variations in results obtained by different investigators are relatively large as shown in Col. B of Table 2. Although the standard deviations are large (averaging ±22% of the means), the values in Col. C selected for calculations of C_b (Col. F) and V_{xg} (Col. G) are close to the mean values of Col. B and in all cases they are well within standard deviations reported by the various investigators.

The values of C_b and V_{xg} calculated by Eq. 5 and listed in Columns E and F of Table 2 determine the absorption rate of exogenous glucose (J_g) in terms of its transcellular and paracellular components. Thus,

$$J_g = V_{xg}\, C_b/(C_b + K_m) + (1 - \sigma)\phi J_v\, C_b \qquad (8)$$
flux = transcellular + paracellular

where V_{xg} = maximum rate of transcellular transport of glucose, μmol hr^{-1} cm^{-2}, K_{mg} = Michaelis-Menten constant of the carrier, mM. $(1 - \sigma)\phi$ for glucose is approximately 0.7 (Fig. 1). Equation 8 contains two unknown constants, namely V_{xg} and K_m. To solve for these constants it is only necessary to determine the unique value

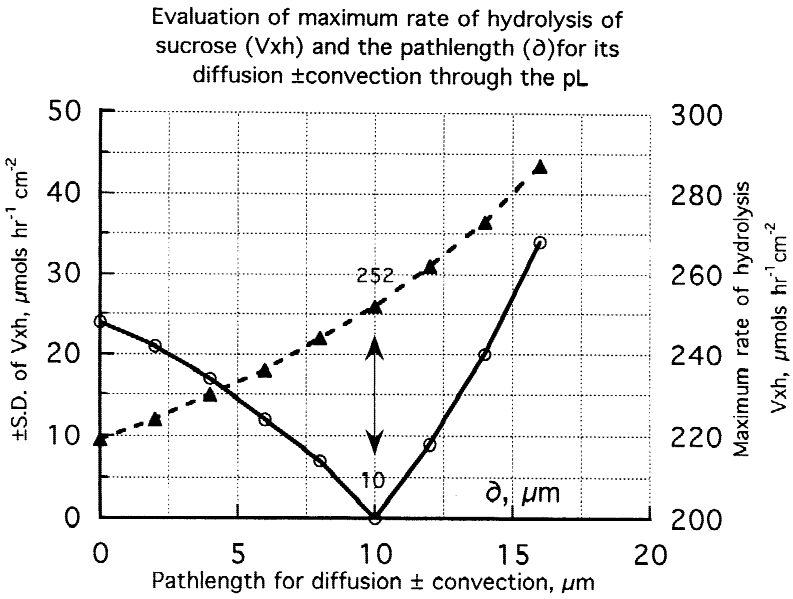

Fig. 4. Evaluation of the maximum rate of hydrolysis of sucrose (V_{xh}, dashed line, right ordinate) and the pathlength (∂) for its diffusion ± convection through pre-epithelial layers. The flux and hydrolysis equations are solved for the unique value of ∂ (10 μm) at which V_{xh} is constant (252 ± 0) at all concentrations of sucrose between 10 and 160 mM.

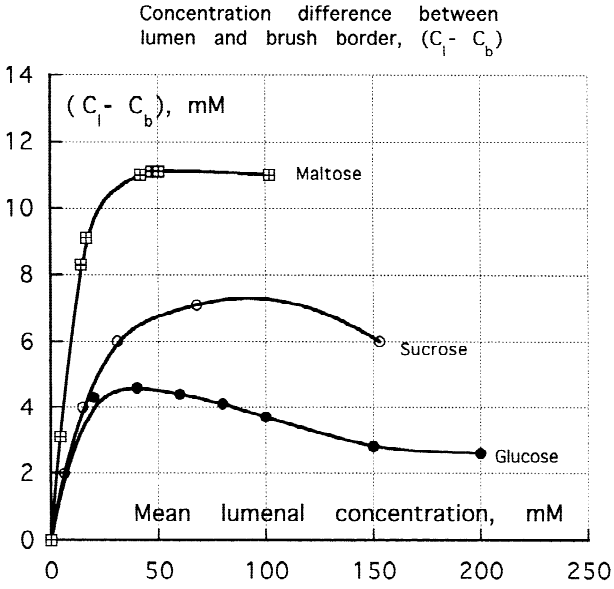

Fig. 5. Concentration differences between lumen and brush border during perfusions of jejunum with glucose, sucrose or maltose. Once the value of ∂ has been established as in Table 1 the concentration of perfused solute in the brush border can be calculated from Eq. 7 for any given lumenal concentration. The values for C_b shown in Table 1, Col. F and Table 2, Col. E are plotted in Fig. 5 which forms the basis for extension of theory to estimate proximal-distal concentrations of hydrolysis products and the kinetic advantage of transporting hexoses from lumen to brush border in the form of saccharides.

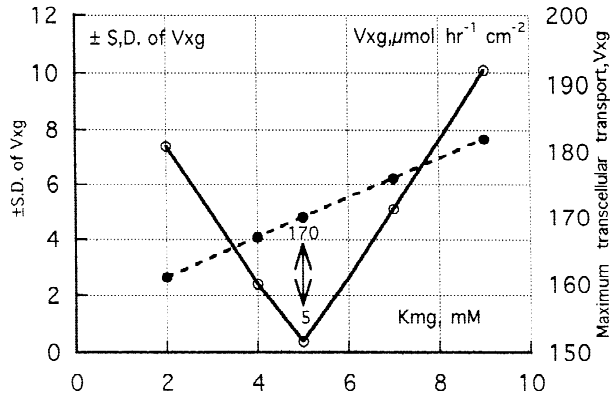

Fig. 6. Evaluation of maximum transcellular transport rate of glucose (V_{xg}) and K_{mg} of apical transporter. It is evident from Fig. 1 that there is no maximum to glucose transport in the physiological range of sugar concentrations. Nevertheless, the transcellular transport maximum (V_{xg}) can be evaluated from the flux data by finding the unique value of K_m at which V_{xg} in Eq. 8 remains constant at all values of perfused glucose concentration. This occurs when $K_{mg} = 5$ mM and $V_{xg} = 170$ as shown in Table 2 and in Fig. 6 above. Dashed line = Solid line =

of K_m that leads to minimum variation of V_{xg} as a function of C_b in Eq. 8. The method of calculation is the same as that used in the previous section to find the unique value of ∂ that leads to a constant value of V_{xh} as a function of concentration. In human perfused jejunum a constant V_{xg} of 170 ± 0 μmols hr^{-1} cm^{-2} occurs at a K_{mg} of 5 mM for brush border concentrations (C_b) ranging from 16–197 mM as shown in Table 2 (Col E and F) and in Fig. 6. Slightly different combinations of K_m and J_g also result in almost constant V_{xg} but the values listed in Table 2 provide the best fit to the experimentally determined means of J_g shown in Col. B. The K_{mg} determined in this way from glucose absorption rates in perfused human jejunum does not differ significantly from the K_{mg} of 4.1 ± 1.7 mM found by Dorando & Crane [13] in membrane vesicles prepared from rabbit jejunum. Given these parameters {i.e., $V_{xg} = 170$, $K_{mg} = 5$ and $(1 - \sigma)\phi = 0.7$} Equation 8 predicts within standard

Table 2. Glucose transport

A	B J_g* μmol/hr/sq cm	C J_g, selected μmol/hr/sq cm	D J_v ml/hr/sq cm	E C_{bg} (Eq. 7) m*M*	F V_{xg} for K_m = 5 m*M* (Eq. 8) μmol/hr/sq. cm
20	130 ± 30	140	0.9	16.1	170
40	185 ± 42	190	1.6	36.0	170
60	230 ± 51	227	1.8	56.2	170
80	260 ± 57	256	1.8	76.4	170
100	290 ± 64	291	1.9	96.8	170
150	360 ± 80	361	1.9	147.6	170
200	430 ± 95	388	1.6	197.8	170
				Mean	170
				±SD	0

Brush border concentrations (C_{bg}) and transcellular transport maxima (V_{xg}) of exogenous glucose perfused through jejunal segments of normal humans.

D = 0.032 sq. cm/hr; ∂ = 10 μm J_g selected to result in constant V_{mxg}.

* Means and average *SD* from ref [15,17,18,19,20,22,29,41,64].

errors of measurement the observed rates of absorption of glucose as a function of its concentration in the brush border of the human jejunum.

The values for C_b at any given flux or lumenal concentration of glucose shown in Table 2 provide the starting point for estimating the pathlength for diffusion–convection from the brush border to lumenal perfusion fluid as described in Part II below.

Part II

Proximal-Distal Concentrations and Fluxes of Free Hexoses During Perfusions of Jejunum with Maltose or Sucrose: The Pathlength for Diffusion ± Convection of Hexoses from Brush Border to Perfusion Fluid

Free glucose (or fructose) generated in the brush border has three possible transport pathways:

(i) It can be captured by membrane bound carriers and enter the transcellular pathway to villus capillary blood

(ii) It can be entrained in paracellular fluid absorption to villus capillary blood.

(iii) It can diffuse back to lumenal perfusion fluid from which it is subject to absorption to blood in more distal regions of the segment.

The jejunal segments used for perfusion experiments are usually so short that substantial quantities of the hydrolytic products are lost to the perfusion outflow via pathway (iii). For example, during perfusion of 15–30 cm lengths of human jejunum with 80 mM sucrose about 50% of the liberated fructose was lost to the perfusion fluid [21, 22] (*see also* Fig. 9 below). Similarly, large quantities of free glucose appear in the outflow during perfusions with maltose [32, 44, 57]. At high concentrations of perfused maltose the "coupling coefficient" (defined as the ratio of glucose absorbed to that hydrolyzed) may be less than 0.5 both in humans [44] and rats [27]. Normally all or most of the hydrolysis products that diffuse from brush border to the lumen in proximal jejunum are carried by intestinal secretions and peristalsis to distal jejunum or upper ileum from which they are absorbed, even during digestion of large loads of saccharides [1, 9, 14, 55]. Nevertheless, an understanding of factors that determine the loss to proximal lumen of hydrolytic products formed in the brush border is necessary for interpretation of results obtained during experimental segmental perfusions.

The rates of brush border hydrolysis and the subsequent fluxes of hydrolytic products through each of the three possible pathways can each be described by relatively simple and well-known equations that apply to solutes in free solution. These equations will be used to construct a mathematical model of the system with the aim of predicting proximal-distal concentrations and fluxes of the free hexoses generated in the brush border as a function of the concentration of perfused disaccharides, the perfusion flow rate, the rate of fluid absorption and the pathlength through the pL for diffusion or convection from brush border to lumenal perfusion fluid. The model predicts the proximal-distal concentrations of glucose or fructose during perfusion of human jejunal segments with maltose or sucrose in concentrations ranging from 10–160 mM. The predicted outflow concentrations are close to observed values when the pathlength for diffusion-convection from brush border to lumenal perfusion fluid is in the range 50–150 μm (Mean = 95 ± 9 μm). This pathlength is 10× greater than the pathlength for diffusion + convection of disaccharides from perfusion fluid to brush border and this result supports the hypothesis that pre-epithelial fluid layers provide a protective blanket that minimizes loss to lumen of monomers generated in the brush border of proximal jejunum

Table 3. Proximal-distal concentrations and fluxes of glucose and fructose during perfusion of 15 cm of human jejunum with 40 mM sucrose

C_{si} = 40mM					Q_{in} = 900 ml/hr			V_{xh} = 261 μmol/hr/sq cm			
Cso = 26.4 ± 1.5 mM					An = 9.6 sq cm			V_{xg} = 170 μmol/hr/sq. cm			
A	B	C	D	E	F	G	H	I	J	K	L
A. Glucose											
n	l,cm	$C_{ls(n)}$	$C_{bs(n)}$	A_nJ_v	$A_nJ_{h(n)}$	Q_n	$C_{lg(n-1)}$	$C_{lg(n)}$	$A_nJ_{a(n)}$	$C_{bg(n)}$	Coupling coeff. (n)
1	1.5	38	33	14.0	1613	886	0	0.4	1241	12.2	0.77
2	3.0	37	31	13.8	1588	872	0.42	0.8	1237	12.1	0.78
3	4.5	35	30	13.6	1564	859	0.82	1.2	1232	12.0	0.79
4	6.0	34	29	13.3	1541	845	1.21	1.6	1228	11.9	0.80
5	7.5	32	28	13.0	1517	832	1.58	1.9	1223	11.9	0.81
6	9.0	31	27	12.8	1494	820	1.93	2.3	1218	11.7	0.82
7	10.5	30	26	12.6	1480	807	2.27	2.6	1222	11.9	0.83
8	12.0	29	25	12.4	1449	795	2.59	2.9	1208	11.5	0.83
9	13.5	28	24	12.2	1427	782	2.89	3.2	1203	11.4	0.84
10	15.0	26	22	12.0	1389	770	3.18	3.4	1219	11.9	0.88
							Observed = 3.1 ± .6				
B. Fructose											
1	1.5	38	33	14.0	1613	886	0	1.2	572	34.32	0.65
2	3.0	37	31	13.8	1588	872	1.18	2.3	581	34.87	0.67
3	4.5	35	30	13.6	1564	859	2.33	3.5	592	35.49	0.69
4	6.0	34	29	13.3	1541	845	3.46	4.6	601	36.06	0.71
5	7.5	32	28	13.0	1517	832	4.57	5.7	610	36.59	0.73
6	9.0	31	27	12.8	1494	820	5.66	6.7	619	37.13	0.76
7	10.5	30	26	12.6	1480	807	6.73	7.8	637	38.22	0.79
8	12.0	29	25	12.4	1449	795	7.78	8.8	637	38.23	0.80
9	13.5	28	24	12.2	1427	782	8.80	9.8	643	38.55	0.82
10	15.0	26	22	12.0	1389	770	9.80	10.8	621	37.26	0.81
							Observed = 10.8 ± .8				

Calculations are for pathlength of 100 μm from brush border to lumen.
Data of Gray & Ingelfinger [22], [*see* text for definition of symbols].

while at the same time offering little impediment to the passage of saccharides (or oligopeptides) from lumen to brush border.

The equations describing flux through each of the three possible pathways include both quadratic and exponential terms and numerical solutions for their combination are complex. Doubtless a fully computerized program could be devised to accomplish this but the solution used by the author involves a tedious process of graphical integration that is only partially automated. For this reason, only the fundamental equations and the principal results obtained from them will be described in the text. A detailed, step-by-step description of the graphical integration process with associated spreadsheets similar to those of Table 3, 4 and 6 are available from the author on request. Success of the model in predicting the simultaneous outflow concentrations of hydrolytic products having such different absorption mechanisms as glucose and fructose over a wide range of sucrose or maltose concentrations lends credibility to the model and its several applications to mechanisms of intestinal absorption of saccharides and oligopeptides.

Units and Definition of Symbols

Most of the symbols to be used in Part II have already been defined in Part I but they are listed here in tabular form for easy reference.

A = area of lumenal surface, cm^2;
C = concentration, μmol cm^{-3};
D = free aqueous diffusion coefficient, cm^2 hr^{-1};
∂^* = pathlength for diffusion ± convection from brush border to perfusion fluid, μm;
J_a = absorptive flux to blood, μmol hr^{-1} cm^{-2};
J_h = rate of hydrolysis of disaccharide, μmol hr^{-1} cm^{-2};
J_l = flux from brush border to lumenal perfusion fluid, μmol hr^{-1} cm^{-2};
$\pm J_v$ = net fluid absorption or secretion, ml hr^{-1} cm^{-2};
ϕ = fraction of net fluid absorption that occurs paracellularly;
ℓ = distance along segment, cm;
K_m = Michaelis-Menten constant for hydrolysis or for carrier transport;
Q = flow of perfusion fluid, ml hr^{-1};
σ = osmotic reflection coefficient;

V_{xhs} = max. rate of hydrolysis of the disaccharide, μmol hr^{-1} cm^{-2};
V_{xg} = max. rate of transcellular carrier transport of glucose, μmol hr^{-1} cm^{-2}.

Subscripts:

$n \approx$ the nth section of the perfused segment
$b \approx$ brush border
$f \approx$ fructose
$g \approx$ glucose
$i,o \approx$ inflow, outflow
$L \approx$ lumenal perfusion fluid
$s \approx$ saccharide

For example $C_{bs(n)}$ denotes the concentration of unhydrolyzed disaccharide in the brush border of the nth section of the perfused segment.

Assumptions Regarding the Concentrations of Unhydrolyzed Disaccharides

At any point in the proximal-distal axis (i.e., in any given sector, n) the concentration of disaccharide in the brush border ($C_{bs(n)}$) is related to its concentration in lumenal perfusion fluid ($C_{Ls(n)}$) by Eq. 7 of Part I and is expressed numerically by the smooth curves shown in Fig. 5. C_L is assumed to decrease exponentially with distance as described in Part I (Fig. 2) but at any point in the proximal-distal axis is assumed to be uniform from the central axis to the pre-epithelial layer.

Let the perfused segment be divided into n sections such that each section has a lumenal surface of A_n cm^2. The rate of hydrolysis in section "n" is then

$$J_{h(n)} = A_n V_{xhs}\, C_{bs(n)}/\{C_{bs(n)} + K_{ms}\} \tag{9}$$

where $C_{bs(n)}$ is the concentration of the saccharide in the nth section of the brush border and K_{ms} is the Michaelis-Menten constant determined in vitro. V_{xh} in perfused segments of human jejunum is 252 μmol hr^{-1} cm^{-2} for sucrose and 266 μmol hr^{-1} cm^{-2} for maltose (Part I, Table I). In vitro determinations of K_{ms} are in the range 3 ± 1 mM for maltose and 18–20 mM for sucrose [1, 24]. In the following analysis we assume that K_{ms} is 3.3 mM for maltose and 18 mM for sucrose.

The glucose or fructose from hydrolysis in the brush border is either absorbed to blood (J_a) or diffuses back to lumenal perfusion fluid (J_L). Hydrolysis of 1 mol of maltose generates 2 mols of glucose for transport, whence

$$J_{a(n)} + J_{L(n)} = 2J_{h(n)} \tag{10}$$

Hydrolysis of 1 mol of sucrose generates 1 mol of glucose and 1 mol fructose whence

$$J_{a(n)} + J_{L(n)} = J_{h(n)} \tag{10a}$$

The rate absorption of *glucose* from brush border to blood in the nth section is

$$J_{ag(n)} = A_n V_{xg}\, C_{bg(n)}/(C_{bg(n)} + K_{mg}) + (1 - \sigma)\phi\, A_n J_v C_{bg(n)}. \tag{11}$$

[see also Eq. 8 of Part I]

The rate of absorption of *fructose* from perfused segments of human jejunum is approximately proportional to its concentration in the perfusion fluid as found experimentally by Holdsworth and Dawson [29] and by Gray and Ingelfinger [22]. The constant of proportionality is 1.7 ± 0.2 μmols hr^{-1} cm^{-2} mM^{-1}. Since the path-length for diffusion-convection in the direction lumen to brush border is only about 10 μm (*see* Table 1 of Part I) the concentration differences are negligible and within experimental error

$$J_{af(n)} = 1.7\, C_{bf(n)} \tag{11a}$$

The rate of diffusion − convection of glucose or fructose from brush border through pre-epithelial layers to perfusion fluid is

$$J_{L(n)} = J_v\{C_L\, e^{(Jv\partial/D)} - C_{b(n)}\}/\{e^{(Jv\partial/D)} - 1\} \tag{12}$$

$$J_{L(n)} = \{A_{(n)}D/\partial^*\}\{C_{b(n)} - C_{L(n)}\} - A_n J_v C_{L(n)}. \tag{12a}$$

Finally, the flux of glucose or fructose from brush border into perfusion fluid of the nth section is also

$$J_{I(n)} = Q_n\{C_{L(n)} - C_{L(n-1)}\} \tag{13}$$

where $Q_n = \{Q_{(n-1)} - J_{v(n)}\}$, $cm^3 hr^{-1}$

Equations 11, 12 and 13 each include a convective component, J_v, which varies with lumenal concentrations of glucose or disaccharide as shown in Fig. 3. Although the experimental data of Fig. 3 have large standard deviations, the mean values for J_v taken from the smooth curve lead to good agreement between theory and experiment as shown below in Fig. 7.

Equations 9–13 contain 6 unknowns, namely $C_{L(n)}$, $C_{b(n)}$, $J_{h(n)}$, $J_{a(n)}$, $J_{L(n)}$ and ∂^*. For any assumed value of ∂^* it is therefore possible to solve for the other five unknowns.

When the selected (assumed) value of ∂^* is such as

Table 4. Proximal-distal concentrations and fluxes of glucose during perfusion of 30 cm of human jejunum with 35 or 69.5 mM maltose

A. C_{in} = 35 mM C_{out} = 9.9 Q_{in} = 1200 ml/hr An = 6.4 sq. cm/cm
V_{xh} = 266 μmols/hr/sq cm V_{xg} = 170 μmols/hr/sq cm

A	B	C	D	E	F	G	H	I	J	K	L
n	l	$C_{ml(n)}$	$C_{mb(n)}$	A_nJ_v	$J_{h(n)}$	Q_n	$C_{(n-1)}$	C_n	$J_{a(n)}$	C_b	coupling coeff.
1	3.0	30.7	19.5	33.00	4368	1167	0.00	3.5	4693	71	0.54
2	6.0	26.9	16.5	29.00	4256	1138	3.46	6.9	4571	74	0.54
3	9.0	23.6	13.2	27.00	4086	1111	6.93	10.3	4476	75	0.55
4	12.0	20.7	10.7	26.00	3903	1085	10.25	13.4	4411	74	0.57
5	15.0	18.1	9.0	25.00	3737	1060	13.38	16.3	4351	74	0.58
6	18.0	15.9	7.0	24.00	3471	1036	16.33	18.9	4231	70	0.61
7	21.0	14.0	5.5	23.00	3192	1013	18.94	21.2	4103	66	0.64
8	24.0	12.2	4.7	22.00	3000	991	21.20	23.2	4012	64	0.67
9	27.0	10.7	4.2	21.00	2860	970	23.20	25.0	3942	63	0.69
10	30.0	9.4	3.8	19.00	2733	951	25.03	26.7	3840	62	0.70
						Observed = 23.2 ± 8.3					

B. C_{in} = 69.5 M C_{out} = 36

n	l	$C_{ml(n)}$	$C_{mb(n)}$	J_v	$J_{h(n)}$	Q_n	$C_{l(n-1)}$	$C_{l(n)}$	$J_{a(n)}$	C_{bg}	coupling coeff.
1	3.0	65.1	54.1	36.00	4813	1184	0.00	3.8	5088	80	0.53
2	6.0	60.9	49.9	35.70	4790	1148	3.83	7.7	5175	84	0.54
3	9.0	57.1	46.1	35.30	4766	1113	7.67	11.5	5257	88	0.55
4	12.0	53.4	42.4	35.00	4739	1078	11.51	15.4	5338	92	0.56
5	15.0	50.0	39.0	34.70	4709	1043	15.35	19.2	5417	95	0.58
6	18.0	46.9	35.9	34.30	4677	1009	19.19	23.0	5484	99	0.59
7	21.0	43.9	32.9	34.00	4641	975	23.02	26.8	5553	103	0.60
8	24.0	41.1	30.1	33.70	4602	941	26.85	30.7	5618	106	0.61
9	27.0	38.5	27.5	33.30	4559	908	30.66	34.5	5669	109	0.62
10	30.0	36.0	25.0	33.00	4512	875	34.45	38.2	5725	113	0.63
							Observed = 36 ± 11				

Calculations are for pathlength of 100 μm from brush border to lumen; Data from McMichael et al. [44].

to predict hexose concentrations in the outflow (i.e., glucose or fructose in the last section) that equal the concentrations actually measured experimentally then the numerical values of the other 5 unknowns are defined and the problem is solved.

Application to Perfusion of Jejunal Segments

Table 3 shows the predicted proximal-distal concentrations and fluxes of glucose and fructose during perfusions of 15 cm segments of human jejunum with 40 mM sucrose at the rate of 900 ml hr^{-1}. This rate of perfusion supplies 36 mmols hr^{-1} of CHO or the caloric equivalent of about 50% of the average energy consumption of a normal 70 kg human; it is therefore well within physiological limits. The calculations in Table 3 assume a pathlength of 100 μm for diffusion-convection of glucose or fructose from the brush border (where they are generated) to the lumenal perfusion fluid. This assumed pathlength results in calculated outflow concentrations (Col. I, n = 10) that are within the standard errors of observed values. Table 4 summarizes analogous data for perfusions of 30 cm segments with 35 or 69.5 mM maltose at the rate of 1,200 ml hr^{-1}. As shown in Col. I, n = 10 the calculated values are within the standard errors of measurement of observed values. Similar calculations for perfusions with 10, 20, 80 and 160 mM sucrose or 28, 80 and 139 mM maltose yield similar results; the pathlengths at which calculated outflows equal observed range from 50–150 μm with a mean of 95 ± 9 (SE) μm. The calculations of Tables 3 and 4 utilize the approximate form of the diffusion-convection equation (Eq. 12a). If the full equation (Eq. 12) is used the average calculated ∂^* is 89 ± 6 μm instead of 95 ± 9 μm.

Figure 7 summarizes the relations between calculated and observed outflow concentrations of free glucose and fructose when the pathlength for their diffusion-convection is 100 μm. Given this pathlength, the theory predicts outflow concentrations of glucose and fructose within experimental errors over the whole range of inflow concentrations of sucrose or maltose (10–160 mM) for 15–30 cm segments of proximal jejunum (distance between catheter sampling sites).

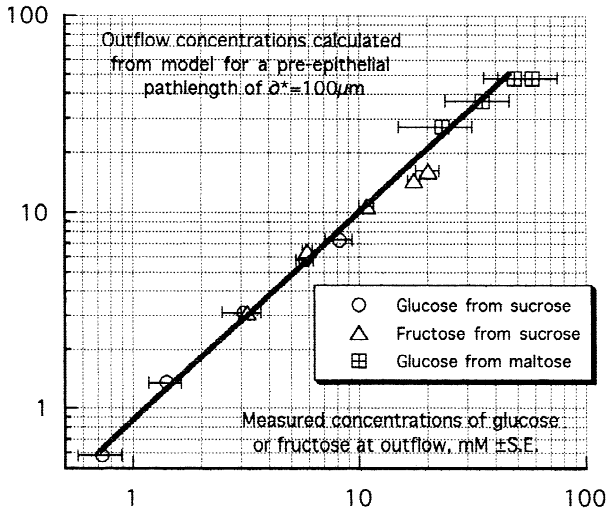

Fig. 7. Predicted outflow concentrations of glucose and fructose during perfusion with sucrose or maltose (10–160 mM) when the pathlength for diffusion minus convection from brush border to perfusion fluid is 100 μm. The predicted concentrations fall within the standard errors of observed values over the entire range of concentrations.

Tables 3 and 4 also show the calculated proximal-distal coupling coefficients (i.e., the ratios of absorption to hydrolysis). For the relatively short segments of proximal jejunum employed by most investigators the losses of hydrolysis products to perfusion fluid may be as high as 36% for glucose and 55% for fructose. It is well known, however, that there is little free glucose in samples of chyme taken from distal regions of the intact jejunum, even after ingestion or perfusion of large loads of maltose or sucrose [4, 8, 14, 55]. In humans more than 80% of large loads of ingested CHO [4] or perfused sucrose and/or glucose [35] are absorbed from the duodenum and the proximal half of the jejunum. It is therefore pertinent to extend the theoretical model to the full length of the jejunum and to examine the role of pre-epithelial fluid layers in minimizing diffusional losses of monomers generated in the brush border.

Extension of Theory to Predict Proximal-Distal Concentrations and Fluxes of Glucose (or Fructose) Over the Full Length of the Jejunum

The equations derived above for predicting proximal-distal fluxes and concentrations assume constant values for maximal rates of hydrolysis of disaccharides (V_{xh}) and maximal rates of transcellular transport of glucose (V_{xg}) per unit area. No systematic studies have been made to determine if maximal rates of hydrolysis or absorption are the same in distal jejunum as they are in proximal jejunum. However, Gray and Ingelfinger [22] found no significant differences in absorption rates of 73 mM exogenous glucose (e.g., 45 ± 5 mmols/hr in distal half of jejunum as compared with 44 ± 4 mmols/hr in proximal half). There was a slightly greater hydrolysis and absorption rate of 73 mmol sucrose in the distal half of jejunum (48 ± 5 mmols/hr) as compared with the proximal (40 ± 4). For purposes of the following analysis it will therefore be assumed that values for maximum rates of hydrolysis of disaccharides (V_{xh}) and transcellular transport of glucose (V_{xg}) evaluated as in Tables 1 and 2 do not vary significantly over the whole length of the human jejunum.

Figure 8 *A* and *B* show the predicted proximal-distal concentrations of lumenal free glucose or fructose during perfusions of the jejunum with 80 mM maltose or sucrose at the rate of 900 ml hr^{-1} (72 mmols hr^{-1} or the caloric equivalent of 2400 kCal/24 hr). The calculations are similar to those illustrated in Table 4 but are based on the data of Gray & Santiago [23] for an inflow of 80 mM maltose. It is assumed that the pathlength for diffusion-convection of glucose from the brush border to the perfusion fluid is 100 μm as determined in the preceding section. The concentrations rise to a maximum of 60 mM at a catheter length of 50 cm or about two-thirds of the distance from the ligament of Treitz to the ileo-cecal valve. The concentrations of free glucose then decrease with distance as glucose carried from more proximal regions is absorbed faster than fresh glucose is formed by the diminishing concentrations of maltose. When concentration is maximal the "coupling coefficient" becomes unity (i.e., the rate of absorption equals rate of presentation to the brush border). The elliptical marker at 30 cm distance is the mean ± SE of the glucose concentration measured experimentally by Gray and Santiago [23]; it falls almost exactly on the predicted curve. Although the concentrations of glucose in distal regions are relatively high the total quantity of glucose lost to perfusion fluid is small owing to concomitant absorption of perfusion fluid. As indicated in Fig. 8 about 70% of the perfusion flow has been absorbed by the time the fluid reaches 60 cm from the ligament of Treitz and the percentage of free glucose lost to the perfusion diminishes from 50% at the inflow to less than 15% at the outflow. The quantity of glucose lost to perfusion fluid includes the glucose remaining in the lumen during steady state perfusion as well as the quantity lost in the distal outflow. In the example of Fig. 8 the integrated estimate of glucose formed by hydrolysis of maltose was about 135 mmols hr^{-1} of which 105 mmols hr^{-1} was absorbed to blood, 18 mmols hr^{-1} was lost in distal perfusate and 11 mmols were present in the intestinal lumen in the steady state of perfusion.

Fructose is absorbed less rapidly than D-glucose and for this reason its (predicted) concentrations continue to increase for the full length of the jejunum during perfusions with 80 mM sucrose as shown in Fig. 8*B*. Of the fructose derived from hydrolysis of perfused sucrose (67 mmols hr^{-1}) the model predicts that about 75% would be absorbed and 25% would be lost to the jejunal perfusion fluid.

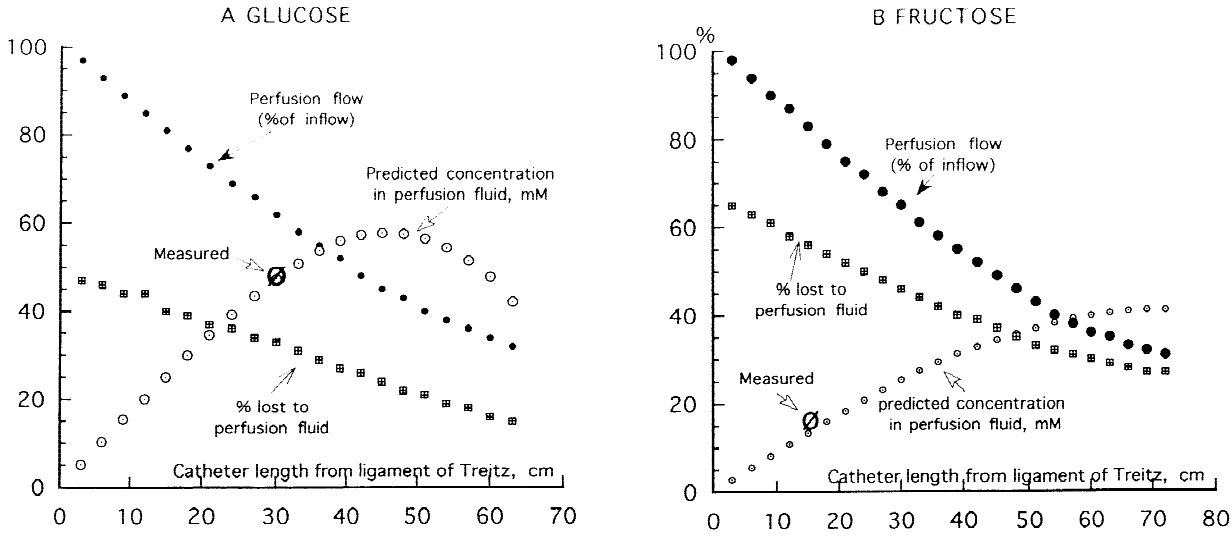

Fig. 8. Predicted diffusion of (*A*) glucose and (*B*) fructose from brush border to lumen (pathlength 100 μm) during perfusion at 900 ml hr^{-1} with 80 mM maltose (*A*) or 80 mM sucrose (*B*); extension of model to full length of jejunum (catheter length 70 cm). The predicted concentration of glucose (*A*) reaches a maximum about 2/3rds of the distance along the jejunum and at this point the absorption to blood exactly matches the presentation to the brush border from proximal perfusion fluid plus local hydrolysis of maltose (i.e., the coupling coefficient = 1.0). The predicted concentration of free glucose at 30 cm exactly matches the concentration found experimentally by Gray & Santiago [23]. Fructose (*B*) is absorbed less rapidly than glucose and in contrast to glucose (*A*) its concentration increases along the full length of the jejunum. The predicted concentration of fructose and its percent loss to perfusion fluid at 15 cm are almost exactly equal to the values measured by Gray & Ingelfinger [22]. The (predicted) loss of fructose to perfusion fluid near the distal end of the jejunum is 27% of the inflow.

Role of Pre-epithelial Layers in Minimizing Losses to Lumen of Hydrolysis Products Formed in the Brush Border

In preceding paragraphs evidence was presented that in perfused segments of jejunum the functional pathlength for diffusion + convection of disaccharides from lumen to brush border is only about 10 μm, whereas the pathlength for diffusion-convection of their hydrolytic products (glucose or sucrose) from brush border to lumen is 50–150 μm (mean = 95 ± 9 μm). This asymmetry raises the possibility that the pre-epithelial ("unstirred") layers covering the brush border might serve a useful function by reducing losses of hydrolytic products to the lumen with corresponding increases in their absorption to blood as first suggested by Gruzdkov [26]. This possibility can now be examined quantitatively by calculating the concentrations and fluxes expected if a pathlength of $\partial^* = 10$ μm is substituted for $\partial^* = 100$ μm in the diffusion-convection equations.

Figure 9*B* shows the predicted losses of fructose during perfusions with 80 mM sucrose if the pathlength for diffusion-convection were only 10 μm as compared with the 100 μm estimated for normal perfused jejunum. For short segments (e.g., 15 cm) the predicted loss of fructose for a pathlength of 10 μm is about 85% as compared with about 50% for 100 μm; the predicted loss over the full length of jejunum is about 35% as compared with 25% for the normal jejunum. In both cases these relatively small amounts of fructose in distal jejunum would probably be fully absorbed to blood as fluid passes along the ileum. In proximal jejunum, however, the pre-epithelial layers evidently provide a significant diffusion barrier that minimizes losses of fructose generated by large loads of sucrose as shown in Fig. 9*B*.

The glucose liberated by hydrolysis of sucrose is absorbed more rapidly than the equimolar fructose and the predicted losses of glucose in distal jejunum are too small to be of physiological significance even if the diffusion-convection pathway from brush border to lumenal perfusion fluid were only 10 μm. For small loads of sucrose (e.g., less than about 50 mmols hr^{-1} inflow) the distal losses of fructose are also too small to be of physiological significance. During perfusions with 80 mM maltose, however, the production of free glucose is more than double that from sucrose and losses of glucose to perfusion fluid are significant. Figure 9*A* shows the predicted losses of glucose during perfusions with 80 mM maltose when the pathlengths for diffusion-convection through pre-epithelial layers are either 100 μm or 10 μm. Under these conditions the 100 μm pathlength minimizes losses of glucose to lumenal fluid in proximal jejunum but the losses are small by the time perfusion fluid reaches distal jejunum.

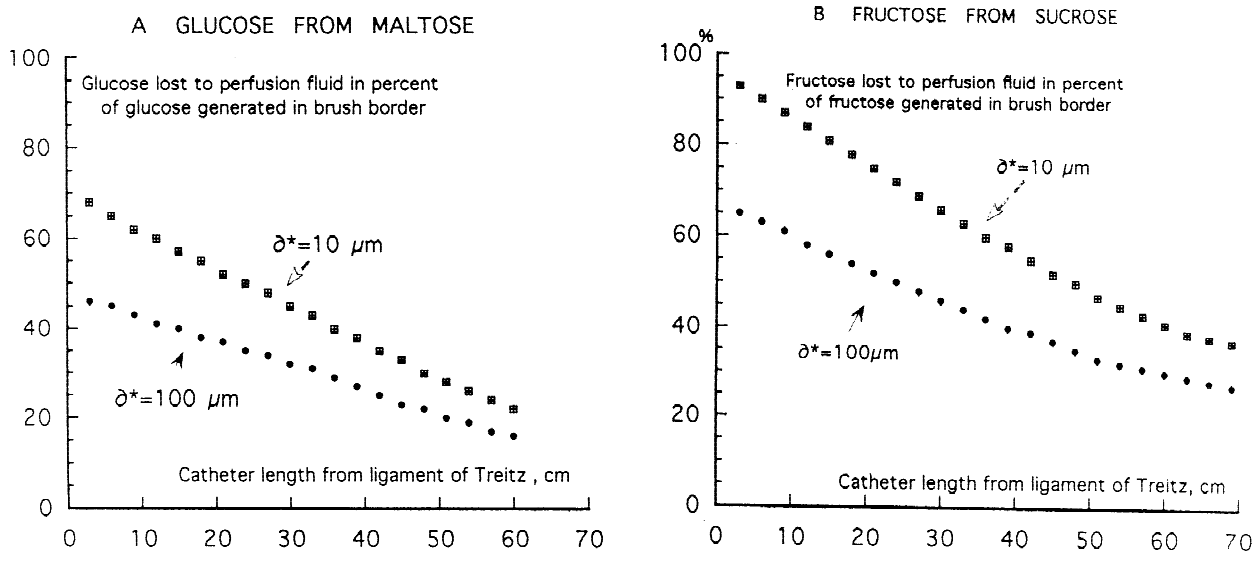

Fig. 9. Effect of pathlength (∂^*) on (*A*) loss of glucose during perfusion with 80 mM maltose or (*B*) loss of fructose during perfusion with 80 mM sucrose. A pathlength of 100 μm for diffusion minus convection provides significant protection against loss of hydrolysis products to lumen when compared with a pathlength of 10 μm for diffusion plus convection of disaccharides in the opposite direction. Despite the complexity of the flux and hydrolysis equations the percentage loss of hydrolysis products is almost linearly related to distance along the jejunum.

Flux of Saccharides Relative to Free Glucose: Does the pL Provide a Kinetic Advantage for Delivery of Glucose Packaged as Saccharides?

Crane and associates [6, 42] were the first to note that more glucose could be absorbed when presented to the mucosa in the form of maltose than as free glucose. The phenomenon was aptly described as a "kinetic advantage" but no credible mechanism was proposed to explain it. In the introduction to the present paper it was pointed out that for a given molar concentration gradient the diffusive flux of monomers bound as oligomers is theoretically proportional to the square root of the molecular weight of the parent oligomer. Thus, in the absence of convective transport, the diffusional flux of a given molar gradient of glucose in the form of maltose is theoretically 37% greater than in the form of free glucose; for a 9 unit oligomer of glucose the diffusional flux of glucose units is theoretically 3× that of free glucose.

Crane's experiments were performed on isolated segments of hamster intestine in which the main component of flux through the pL was diffusive and the diffusion pathway was abnormally long compared to in vivo conditions. However, several investigators have reported that maltose [32, 57], maltotriose [32] or partial hydrolysates of starch [31, 68] are absorbed more efficiently than equicaloric loads of exogenous D-glucose. Similarly, in rats more glycine is absorbed in the form of di-, tri- or tetraglycine than from free exogenous glycine [43]. When the data of Fig. 1 are replotted in terms of glucose units as in Fig. 10 it becomes clear that glucose bound in the form of maltose is absorbed more rapidly than equal caloric loads of exogenous free monomer in perfused jejunal segments of humans.[1] The issue is of practical importance for oral rehydration therapy because partial hydrolysates of starch or rice are less expensive and simpler to prepare than pure glucose for large scale clinical use [46, 68].

The qualitative theoretical explanation of this kinetic advantage described in the introduction to the present paper can now be examined quantitatively. Table 5 shows the predicted delivery of glucose units (J) to the brush border when the lumenal glucose is either in the form of free glucose or an isocaloric load of maltose. At equal caloric loads the flux of CHO through the pL in the form of maltose is more than double that of glucose (Col. F). The observed absorption rates (J_a) of glucose generated from maltose are less than the amounts reaching the brush border (Col. G) because some of the brush border glucose derived from maltose is lost to the perfusion fluid as described in the preceding section. Thus the kinetic advantage is less when measured in terms of glucose absorption than when measured as flux of glu-

[1] Unlike other investigators, McMichael et al. [44] concluded that there is no kinetic advantage for absorption of glucose in the form of maltose. However, McMicheal et al. did not compare absorption rates of maltose with those of exogenous glucose in their own experiments. Instead they utilized the glucose data of Holdsworth & Dawson [29] who reported glucose absorption rates that are about 50% higher than those found by numerous subsequent investigators and summarized in Figs. 10 and Table 2 of the present paper.

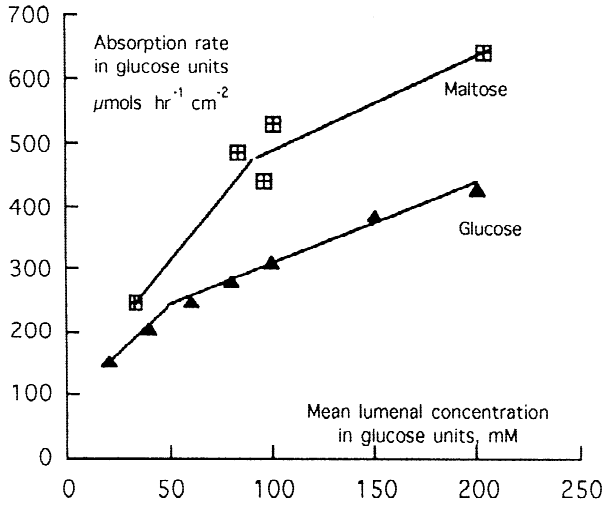

Fig. 10. Experimental demonstration of the kinetic advantage to transport of glucose across pre-epithelial layers in the form of disaccharide rather than free glucose. The data are the same as those of Fig. 1 but expressed as glucose units (proportional to grams per liter of CHO) rather than molar concentrations and fluxes. The highest concentration of maltose shown in Fig. 1 is not included because it would be off scale.

cose units through the pL. Application of the model to 1–4 linked saccharides larger than maltose such as those generated by lumenal digestion or by partial hydrolysis of starch can be made on the assumption that the K_m for hydrolysis (3–4 mM) is the same as for maltose [1, 24]. Table 6 and Fig. 11 show the calculated kinetic advantage as a function of number of glucose units in the saccharide. For loads of CHO in the physiological range (up to 100 mmols hr^{-1}) the model predicts a maximum advantage for saccharides having 3–6 glucose units. This prediction appears to be supported, at least qualitatively, by the investigations of Jones et al. [31, 32] who found that maltose and maltotriose confer a greater kinetic advantage to absorption of glucose units than higher molecular weight 1–4 linked saccharides. Calculations utilized for construction of Table 6 and Fig. 11 are shown in Appendix C.

Discussion

Most investigators agree that hexoses or amino acids generated by membrane-bound hydrolases at the surface of absorptive cells can combine with membrane carriers in conformance with the laws of mass action in free solution (Michaelis-Menten kinetics). If this is the case, however, it should follow that hydrolysis products will also be free to diffuse back to the intestinal lumen and in fact large quantities of free hexoses are found in effluents from short intestinal segments perfused with sucrose or maltose both in humans [22, 32, 44, 57] and in rats [27]. Theoretically, if there were no pL ($\partial^* = 0$) the rate of diffusion to lumen of monomers generated in the brush border would be infinite. Unstirred layers may therefore be necessary to prevent undue losses of hydrolytic products and the extent of such losses will be determined by the functional pathlength through the pL to lumen on the one hand and the kinetic properties of transport from brush border to blood on the other. In the present paper I have attempted to combine and evaluate these opposing transport processes. My analysis includes heretofore neglected convectional transport of oligomers through the pL and a paracellular component of their absorption to blood in unhydrolyzed form. When these components of flux are included in the analysis the estimated pathlength for diffusion plus convection of disaccharides from lumenal perfusion fluid to the brush border is only 10 ± 2 μm or little more than the anatomical thickness of the glycocalyx and mucus layers. This is far less than any previous estimates and leads to the conclusion that the pL offers very little resistance to the passage of products of lumenal digestion to sites of final hydrolysis to monomers in the brush border. Hydrolysis at or near cell surfaces provides a sink for maintaining relatively large concentration differences of oligomers across the pL. Thus the molar concentration differences across the pL are larger for maltose or sucrose than they are for exogenous glucose as shown in Fig. 5. Given the added fact (heretofore neglected) that the quantity of monomer reaching the brush border by diffusion (per unit concentration difference) is proportional to the square root of the molecular weight of the parent oligomer, it follows that there will be a considerable kinetic advantage to transport through the pL in the form of oligomers as shown quantitatively in Figs. 10 and 11. Indeed, it may be argued that digestion of carbohydrates or proteins to intermediate sized oligomers in the lumen, followed by final hydrolysis to monomers at cell surfaces under a protective blanket of mucus and unstirred layers is an efficient overall process that developed by natural selection.

There are no enzymes to remove hydrolytic products diffusing from brush border to lumen and the diffusion gradients can extend as far into the lumen as mechanical mixing and proximal-distal flow of chyme flow will allow. According to the proposed model the diffusion distance for glucose or fructose generated in the brush border during perfusions with sucrose or maltose extends 50–150 μm into the perfusion fluid or 5–15× the pathlength for saccharides moving in the opposite direction. From a functional point of view the pL acts as a rectifier with conductance to nutrients in the direction lumen to blood some 10-fold greater than in the opposite direction.

Each of the several flux equations utilized in the present analysis is relatively well known and tested but their combination leads to exponential, hyperbolic and quadratic terms that render numerical solutions difficult. Few readers will wish to invest the hours required to

Table 5. Kinetic advantage for absorption of maltose relative to glucose

A	B C_L, mM (mean)	C C_b From Fig. 5	D Jv From Fig. 3	E exp$Jv(\partial/D)$	F Predicted J from Eq. 6	G Observed J_a from Fig. 10
Glu	30	25.6	1.4	1.0448	180	185
Malt	15	7	1.4	1.0628	399	300
Glu	60	55.6	1.8	1.0579	245	250
Malt	30	19.5	1.8	1.0814	572	380
Glu	100	96.4	1.9	1.0612	302	310
Malt	50	39	1.9	1.0861	675	495
Glu	150	146.2	1.9	1.0612	403	390
Malt	75	64	1.9	1.0861	770	560

Comparison of predicted flux (J) through pL with observed absorption rates to blood (Ja).
J and Ja measured in glucose units, μmol/hr/sq. cm.

Table 6. Kinetic advantage

A	B	C	D	E	F	G	H	I	J
		V_{xh} = 252 μmols/hr/sq cm			∂ = 10 μm	K_m = 3.3 mM		Jsg	
Glucose units	D sq cm/hr	C_L mM	Jv ml/hr/sq cm	$(1-\sigma)\phi$	C_b from Eq. C2 of Appendix C	exp$J_v\partial/D$	Js, Eq. 6	Glucose units	Kinetic advant.%
1	0.032	30	1.4	0.7	25.6	1.0447	180	180	0
2	0.023	15	1.4	0.68	7.6	1.0628	186	372	107
3	0.019	10	1.4	0.65	3.5	1.0765	133	399	122
4	0.017	7.5	1.4	0.63	2.0	1.0858	100	401	123
5	0.015	6	1.4	0.61	1.3	1.0978	76	378	110
6	0.014	5	1.4	0.59	1.0	1.1052	60	362	101
9	0.011	3.3	1.4	0.57	0.5	1.1357	34	302	68
1	0.032	60	1.8	0.7	55.6	1.0579	245	245	0
2	0.023	30	1.8	0.68	20.7	1.0814	260	519	112
3	0.019	20	1.8	0.65	10.4	1.0994	210	630	157
4	0.0167	15	1.8	0.63	5.8	1.1138	173	690	182
5	0.015	12	1.8	0.61	3.6	1.1275	140	701	186
6	0.014	10	1.8	0.59	2.5	1.1372	116	698	185
9	0.011	6.7	1.8	0.57	1.1	1.1778	69	619	153
1	0.032	100	1.9	0.7	96.4	1.0612	302	302	0
2	0.023	50	1.9	0.68	39.6	1.0861	324	649	115
3	0.019	33	1.9	0.65	21.7	1.1052	267	801	165
4	0.0167	25	1.9	0.63	13.4	1.1205	230	922	205
5	0.015	20	1.9	0.61	8.6	1.1350	198	992	229
6	0.014	17	1.9	0.59	6.1	1.1453	175	1049	247
9	0.011	11	1.9	0.57	2.3	1.1885	109	977	224

check the numerical calculations or to test the effects of varying the parameters I have selected from the literature to construct the Tables and illustrations. Analogy may be made to the equations describing flux of respiratory gases in both directions between lungs and blood. The lumenal contents, like the alveolar gases, are outside the body. Exchange of intestinal solutes between lumen and blood involves diffusion, convection and complex reactions with carriers and so, too, does the respiratory gas exchange. Respiratory exchange equations include hyperbolic and logarithmic components as well as the complex reactions of oxygen with its transport protein (hemoglobin). The combination of these equations results in cumbersome relationships which are nevertheless fundamental to understanding respiratory gas exchange in health and disease. As stated by Rahn and Fenn [53] the resulting analysis is ". . . highly forbidding at first acquaintance and even the more mathematically inclined physiologists are inclined to resent this kind of symbolism as an unnecessary complication — and they there-

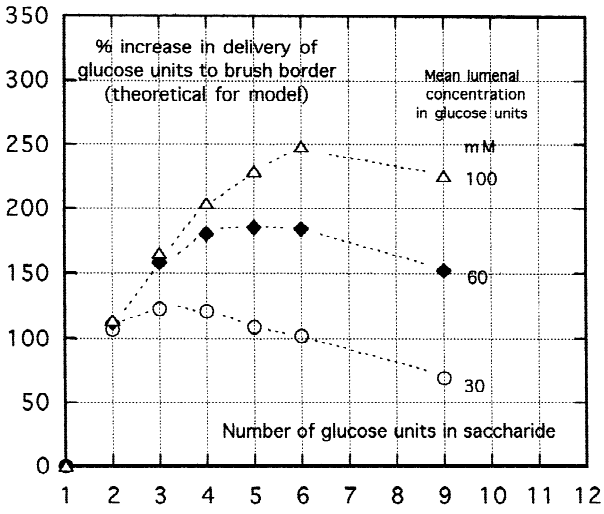

Fig. 11. Prediction of kinetic advantage for delivery of glucose to the brush border in the form of 1–4 linked saccharides rather than isocaloric free glucose. The kinetic advantage depends on two factors (i) for any given molar concentration gradient the number of glucose units transported across the pL by diffusion is proportional to the square root of the molecular weight of the parent saccharide and (ii) the molar concentration gradient of saccharides is greater than that for (exogenous) free glucose by virtue of hydrolysis at the brush border as shown in Fig. 5. The kinetic advantage for diffusion is reduced by convection and the convective component becomes more significant with larger saccharides.

fore put it aside in expectation of the day when the necessary facts can be explained in a few words."

In the present paper I have tried to develop a similar integrative analysis of solute exchanges across the pL of the small intestine in a form that is mathematically correct but is necessarily complex. At the same time I have tried to present the material in qualitative, nonmathematical form in the hope that at least some nonmathematically inclined readers will appreciate its significance and will be stimulated to make use of the several potential applications to mechanisms of intestinal absorption.

I thank Drs. Andrei Gruzdkov and Ludmila Gromova of the Pavlov Institute, St. Petersburg, Russia, for supplying me with translations of their papers and sharing with me the results of extensive, unpublished data obtained from their unique methods for chronic perfusions of jejunal segments in unanesthetized rats. In many ways their results mirror the human data and support the generality of the hypotheses proposed in the present paper.

References

1. Alpers, D.H. Digestion and absorption of carbohydrates and proteins 1987. *In*: Physiology of the Gastrointestinal Tract. (2nd ed). L.R. Johnson, editor. pp. 1469–1487. Raven Press, New York
2. Antoniolli, J.A., Christensen, H.N. 1968. A mode of intestinal absorption unusually dependent on physiological state. *Am. J. Physiol.* **215:**951–958
3. Barry, P.H., Diamond, J.M. 1984. Effects of unstirred layers on membrane phenomena. *Physiol. Rev.* **64:**763–857
4. Borgström, B., Dahlquist, A., Lundh, G., Sjövball, J. 1957. Studies of intestinal digestion and absorption in the human. *J. Clin. Invest.* **36:**1521–1536
5. Chivers, D.J., Hladik, C.M. 1980. Morphology of the gastrointestinal tract in primates: comparisons with other mammals in relation to diet. *J. Morphology* **166:**337–386
6. Crane, R.K. 1975. Fifteen years of struggle with the brush border. *In*: Intestinal Absorption and Malabsorption. T.Z. Czaky, editor. Raven Press, New York
7. Curry, F.E. 1984. Mechanics and thermodynamics of transcapillary exchange. *In*: Handbook of Physiology. The Cardiovascular System. Microcirculation. pp. 309–374. Am. Physiol. Soc., Bethesda, MD
8. Dahlquist, A., Thomson, D.L. 1963. The digestion and absorption of maltose and trehalose by the intact rat. *Acta Physiol. Scand.* **59:**111–125
9. Dahlquist, A., Thomson, D.L. 1963. The digestion and absorption of sucrose by the intact rat. *J. Physiol.* **167:**193–209
10. Dainty, J., House, C.R. 1966. "Unstirred" layers in frog skin. *J. Physiol.* **182:**66–78
11. Dill, D.B., Edwards, H.T., Talbott, J.H. 1932. Studies in muscular activity. *J. Physiol.* **77:**49–62
12. Dillard, R.I., Eastman, H., Fordtran, J.S. 1965. Volume-flow relationship during transport of fluid through the human small intestine. *Gastroenterology* **49:**58–66
13. Dorando, F.C., Crane, R.K. 1984. Studies of the kinetics of Na^+ gradient-coupled glucose transport as found in brush border membrane vesicles from rabbit jejunum. *Biochim. Biophys. Acta* **772:**273–287
14. Ferraris, R.P., Yashapur, S., Lloyd, K.C.K., Mirzayan, R., Diamond, J.M. 1990. Luminal glucose concentrations in the gut under normal conditions. *Am. J. Physiol.* **259:**G822–G837
15. Fine, K.D., Santa Ana, C.A., Porter, J.L., Fordtran, J.S. 1993. Effect of D-glucose on intestinal permeability and its passive absorption in human small intestine in vivo. *Gastroenterology* **105:** 1117–1125
16. Fordtran, J.S., Ingelfinger, F.J. 1968. Absorption of water, electrolytes and sugars from the human gut. *In*: Handbook of Physiology. Alimentary Canal Vol III Intestinal Absorption. pp. 1457–1490 Am. Physiol. Soc., Bethesda, MD
17. Fordtran, J.S. 1975. Stimulation of active and passive sodium absorption by sugars in the human jejunum. *J. Clin. Invest.* **55:**728–737
18. Fordtran, J.S., Saltin, B. 1967. Gastric emptying and intestinal absorption during severe exercise. *J. Appl. Physiol.* **23:**331–335
19. Gisolfi, C.V., Summers, R.W., Schedl, H.P., Bleiler, T.L., Oppliger, R.A. 1990. Human intestinal water absorption: direct vs indirect measurements. *Am. J. Physiol.* **258:**G216–222
20. Gisolfi, C.V., Summers, R.W., Schedl, H.P., Bleiler, T.L. 1992. Intestinal water absorption from select carbohydrate solutions in humans. *J. Appl. Physiol.* **73:**2142–2150
21. Gray, G.M., Ingelfinger, F.J. 1995. Intestinal absorption of sucrose in man: the site of hydrolysis and absorption. *J. Clin. Invest.* **44:**390–397
22. Gray, G.M., Ingelfinger, F.J. 1966. Intestinal absorption of sucrose in man: Interrelation of hydrolysis and monosaccharide product absorption. *J. Clin. Invest.* **45:**388–397
23. Gray, G.M., Santiago, N.A. 1966. Disaccharide absorption in normal and diseased human intestine. *Gastroenterology* **51:**489–498
24. Gray, G.M., Lally, B.C., Conklin, K.A. 1979. Action of intestinal

sucrose-isomaltase and its free monomers on an α-limit Dextrin. *J. Biol. Chem.* **254:**6038–6043
25. Gruzdkov, A.A., Gusev, V., Ugolev, A.M. 1989. Mathematical modelling. *In*: Membrane Digestion: New Facts and Concepts. A.M. Ugolev, editor. pp. 228–234. Mir Publishers, Moscow (English edition)
26. Gruzdkov, A.A. 1993. Modern concepts of substance transfer across the pre-epithelial layer of the small intestine. *Sechenov J. Physiol.* **79:**19–32 (in Russian)
27. Gruzdkov, A.A., Gromova, L.V. 1995. The coupling of disaccharide hydrolysis with absorption of released glucose in the small intestine in vivo. *Dokl. Akad. Nauk.* **342:**830–832 (in Russian)
28. Hallbäck, D.A., Jodal, M., Mannischeff, M., Lundgren, O. 1991. Tissue osmolarity in intestinal villi of four mammals in vivo and in vitro. *Acta Physiol. Scand.* **143:**271–277
29. Holdsworth, C.D., Dawson, A.M. 1964. The absorption of monosaccharides in man. *Clin. Sci.* **27:**371–379
30. International Critical Tables. 1929. Vol. 5. McGraw-Hill Publishing, New York
31. Jones, J.M., Brown, B.E., Loran, J.S., Edgerton, D., Kennedy, J.F., Stead, J.A., Silk, D.B.A. 1983. Glucose absorption from starch hydrolysates in the human jejunum. *Gut* **24:**1152–1160
32. Jones, J.M., Higgins, B.E., Silk, D.B.A. 1987. Glucose absorption from maltotriose and glucose oligomers in the human jejunum. *Clin. Sci.* **72:**409–414
33. Karasov, W.B., Cork, S.J. 1994. Glucose absorption by a nectarivorus bird: the passive pathway is paramount. *Am. J. Physiol.* **267:**G18–G26
34. Kinter, W.B., Wilson, T.H. 1965. Autoradiographic study of sugar and amino acid absorption by everted sacs of hamster intestine. *Cell Biol.* **25:**19–39
35. Lambert, C.F., Chang, R.T., Xia, T., Summers, R.W., Gisolfi, C.V. 1997. Absorption from different intestinal segments during exercise. *J. Appl. Physiol.* **83:**204–212
36. Larner, J., McNickle, C.M. 1955. Products of gastrointestinal starch digestion. *Fed. Proc.* **14:**242
37. Lee, J.S. 1969. A micropuncture study of water transport by dog jejunal villi in vitro. *Am. J. Physiol.* **217:**1528–1533
38. Levey, D.J., Cipollini, M.L. 1996. Is most glucose absorbed passively in Northern Bobwhite? *Comp. Biochem. Physiol.* **113A:** 225–231
39. Levitt, M.D., Fine, C., Ferne, J.K., Levitt, D.G. 1996. Use of maltose hydrolysis measurements to characterize the interaction between the aqueous diffusion barrier and the epithelium in the rat jejunum. *J. Clin. Invest.* **97:**2308–2315
40. Ma, T.Y., Hollander, D., Erickson, R.A., Truong, H., Krugliak, P. 1991. Is the small intestinal epithelium truly "tight" to inulin permeation? *Am. J. Physiol.* **260:**G669–G676
41. Malawer, S.J., Ewton, M., Fordtran, J.S., Ingelfinger, F.J. 1965. Interrelationships between jejunal absorption of sodium, glucose and water in man. *Am. Soc. Clin. Invest.* **44:**1072–1073
42. Malathi, P., Ramaswamy, K., Caspary, W.F., Crane, R.K. 1973. Studies on transport of glucose from disaccharides by hamster small intestine in vitro: I. Evidence for a disaccharide related transport system. *Biochem. Biophys. Acta* **45:**483–489
43. Matthews, D.M., Craft, I.L., Geddes, D.M., Wise, I.J., Hyde, C.W. 1968. Absorption of glycine and glycine peptides from the small intestine of the rat. *Clin. Sci.* **35:**415–424
44. McMichael, H.B., Webb, J., Dawson, A.M. 1967. The absorption of maltose and lactose in man. *Clin. Sci.* **33:**135–145
45. Michel, C.C., Curry, F.E. 1999. Microvascular permeability. *Physiol. Rev.* **79:**703–761
46. Molla, A.M., Hossain, M., Sarker, S.A., Molla, A., Greenough, W.B. 1982. Rice-powder electrolyte solution as oral therapy in diarrhea due to *V. cholerae* and *E. coli. Lancet* 1317–1319
47. Nadel, E.R., Bussolari, S.E. 1988. The Daedalus Project: physiological problems and solutions. *Amer. Scientist* **76:**351–360
48. Pappenheimer, J.R., Reiss, K.Z. 1987. Contribution of solvent drag through paracellular junctions to absorption of nutrients by the small intestine. *J. Membrane Biol.* **100:**123–136
49. Pappenheimer, J.R., Dahl, C.E., Karnovsky, M.L., Maggio, J.E. 1994. Intestinal absorption and excretion of octapeptides composed of D-amino acids. *Proc. Natl. Acad. Sci. USA* **91:**1942–1945
50. Pappenheimer, J.R., Karnovsky, M.L., Maggio, J.E. 1997. Absorption and excretion of undegradable peptides: role of lipid solubility and net charge. *J. Pharm. Exptl. Therap.* **280:**292–300
51. Pappenheimer, J.R. 1998. Scaling of dimensions of small intestines in non-ruminant eutherian mammals and its significance for absorptive mechanisms. *Comp. Biochem. Physiol. A* **121:**45–58
52. Patlak, C.S., Goldstein, D.A., Hoffman, J.F. 1963. The flow of solute and solvent across a two membrane system. *J. Theoret. Biol.* **5:**426–442
53. Rahn, H., Fenn, W.O. 1955. A graphical analysis of the respiratory gas exchange. American Physiological Society, Washington, D.C.
54. Renkin, E.M. 1986. Some consequences of capillary permeability to macromolecules: Starling's hypothesis reconsidered. *Am. J. Physiol.* **250:**H706–710
55. Reynall, P.C., Spray, G.H. 1956. The absorption of glucose by the intact rat. *J. Physiol.* **134:**531–537
56. Sadowski, D.C., Meddings, J.B. 1993. Luminal nutrients alter tight-junction permeability in the rat jejunum: an in vivo perfusion model. *Can. J. Physiol. Pharmacol.* **71:**835–839
57. Sandle, G.I., Lobley, R.W., Holmes, R. 1982. Maltose hydrolysis and absorption in the human jejunum. *Digestion* **24:**137–145
58. Semenza, G. 1986. Anchoring and biosynthesis of stalked brush border membrane proteins: glycosidaser and peptidases of enterocytes and renal tubuli. *Ann. Rev. Cell Biol.* **2:**255–313
59. Shi, X., Summers, R.W., Schedl, H.P., Flanagan, S.W., Chang, R., Gisolfi, C.V. 1995. Effects of carbohydrate type and concentration and osmolality of water absorption. 1995. *Med. Sci. Sports Exerc.* **27:**1607–1615
60. Sjöquist, A., Beeukes, R. 1989. Villous sodium gradient associated with volume absorption in the feline intestine: an electron-microprobe study on freeze-dried tissue. *Acta Physiol. Scand.* **136:**271–279
61. Smithson, K.W., Millar, D.B., Jacobs, L.R., Gray, G.M. 1981. Intestinal diffusion barrier: unstirred water layer or membrane surface coat? *Science* **214:**1241–1243
62. Stevens, C.E. 1988. Comparative Physiology of the Digestive Tract, Chapt. 3. Cambridge University Press
63. Strocchi, A., Corrazza, G., Furne, J., Fine, C., Di Sario, A., Gasbarrini, G., Levitt, M.D. 1996. Measurements of the jejunal unstirred layer in normal subjects and patients with celiac disease. *Am. J. Physiol.* **270:**G487–G491
64. Sladen, G.E., Dawson, A.M. 1969. Interrelationships between the absorptions of glucose, sodium and water by the normal human jejunum. *Clin. Sci.* **36:**119–132
65. Ugolev, A.M., DeLaey, P. 1973. Membrane digestion: a concept of enzyme hydrolysis on cell membranes. *Biochim. Biophys. Acta* **300:**105–128
66. Ugolev, A.M., Zaripov, B.Z., Lezuitova, N.N., Gruzdkov, A.A., Rybin, I.S., Voloshenovich, M.I., Nikitina, A.A., Punin, M.Y., Togoev, N.T. 1986. A revision of current data and views on membrane hydrolysis and transport in the mammalian small intestine based on a comparison of the techniques of chronic and acute experiments: experimental re-investigation and critical review. *Comp. Biochem. Physiol.* **85A:**593–612

67. Ugolev, A.M. 1989. Membrane digestion: new facts and concepts. (English translation) Mir Press, Moscow
68. Zheng, Bai-Yu, Khin-Maung-U, R., Rong-Bao, L., Maiese, R.L., Maiese, S., Lebenthal, E. 1993. Absorption of glucose polymers from rice in oral rehydration solutions by rat small intestines. *Gastroenterology* **104:**81–85

Appendix A

Derivation of Eq. A1 used by Smithson et al. [61] and by Levitt et al. [39, 63].

$$\partial = DA(K'_m - K_m)/0.5\ V'_x \tag{A1}$$

where ∂ = thickness of pre-epithelial layers (pL), D = diffusion coefficient of solute in pL, A = surface area of the pL, V'_x = estimated maxium rate of hydrolysis in the segment, K'_m = apparent Michaelis-Menten affinity of the solute for its enzyme = mean concentration of the solute in the segment when hydrolysis rate is 50% of V'_x, K'_m = Michaelis-Menten affinity of hydrolysis measured in vitro with enzymes purified from intestinal epithelium.

Assumptions

(1) All of the saccharide (or peptide) removed from the perfusate (J_S passes through the pL and is hydrolyzed at a rate J_h in the brush border, i.e., $J_S = J_h$
(2) J_S or J_h approach a maximum value (V_{xh}) at high lumenal concentrations (C_L) and the value of V_{xh} can be determined by extrapolation of experimental data relating J_S to C_L.
(3) When $J_S = J_h = 0.5\ V_{xh}$, $C_L = K'_m$ and $C_b = K_m$ where C_b = concentration of saccharide (or peptide) in the brush border
(4) Transport through the pL is purely diffusive so that

$$J_S = DA/\partial\ (C_L - C_b) \quad \text{or} \quad \partial = DA/J_S\ (C_L - C_b)$$

and substitution of (3) in (4) yields

$$\partial = DA(K'_m - K_m)/0.5\ V'_{xh}\ \text{q.e.d.} \tag{A1}$$

For reasons given in the present paper it appears that all the above assumptions are flawed and the derived values for ∂ have no physiological significance.

Appendix B

Derivation of equations describing steady-state, linear diffusion in the presence of convective flow as applied to pre-epithelial layers (pL) of the small intestine.

The concentrations of saccharides and oligopeptides produced in lumenal fluid by pancreatic amylases and trypsins decrease progressively from duodeum to ileum. However, in any one crosssectional sector (Δl) along the length of the intestine we will assume the concentrations to be homogeneous from the central axis of the lumen up to the functional beginning of the pL. In such a sector the flux of solute arriving at the brush border by diffusion and convection is

$$J_S = J_v\ C_{(x)} + D\ dC/dx \tag{B1}$$

where

J_S = flux of solute per unit area of mucosal surface in the sector
J_V = absorptive flow of the fluid per unit area (velocity of flow),
$C_{(x)}$ = concentration of solute at any distance (x) from the epithelial brush border and
D = diffusion coefficient in the pre-epithelial layers

Equation B1 is similar to that utilized by Dainty & House [10] to describe convective and diffusive transport of NaCl through frog skin.

In the steady state, J_S, is constant and differentiation of Eq. 1 yields

$$0 = J_V\ dC/dx + D\ d^2C/dx^2 \tag{B2}$$

Let $dC/dx = y$ or $dy/y = -(J_V/D)\ dx$ and after integration $y = K_1\ e^{-(Jv/D)x}$.

Substitution of y in Eq (B1) yields

$$J_S = J_V\ C_{(x)} + D\ K_1\ e^{-(Jv/D)x} \tag{B3}$$

When $x = 0$, $C = C_b$, where C_b is concentration of solute at apical membranes of brush border.

$$\text{Whence } K_1 = (J_S - J_V\ C_b)/D \tag{B3a}$$

When $x = \partial$, $C = C_L$ is concentration of solute at the interface between the pre-epithelial layers and well mixed contents of the intestinal chyme in the central lumen.

Substitution in Eq. B3 and B3a and solving for J_S yields

$$J_S = J_V\ \{C_L\ e^{(JV\partial/D)} - C_b\}/\{e^{(JV\partial/D)} - 1\} \tag{B4}$$

Equation B4 was first applied to transport through pL of intestine by Gruzdkov, Gusev & Ugolev (1981) [*see* Ugolev: Membrane Digestion, Mir Press 1989. Eq. 5.2]

When $(Jv/D)\partial$ less than about 0.2, $e^{(Jv/D)\partial} = 1 + (Jv/D)\partial$ (within 2%) and Eqs. B4 and B5 reduce to the familiar forms

$$J_S = D\ (C_L = C_b)/\partial + J_V C_L \tag{B5}$$

flux = diffusion + convection

For diffusion in the direction opposite to convective flow the original differential equations becomes $J_s = J_v\ C_{(x)} - D\ dC/dx$ and the steady state flux becomes

$$J^*_S = J_v\ \{C_b - C_L\ e^{(J_V\partial^*/D)}\}/\{e^{(J_V\partial^*/D)} - 1\} \tag{(6)}$$

where the * refers to flux from brush border to lumen.

Appendix C

Algebraic solution for brush border concentrations of saccharides (C_b) as a function of lumenal concentrations (C_L) using the numerical values for V_{xh}, ∂, and J_V given in Table 1.
(1) From Eq. 4 of the text and Eq. B5 in Appendix B

$$J_S = (V_{mxh}C_b)/(C_b + K_m) + (1 - \sigma)\phi\ J_V C_b = D\ (C_L - C_b)/\partial + J_V C_L \tag{C1}$$

(2) Setting $\{(1 - \sigma)\phi\ JV + D/\partial\}/(J_V + D/\partial)\} = A$, $[V_{maxH}/(J_V + D/\partial) + (K_m - C_L)] = B$ and solving the resultant quadratic for C_b

$$C_b = \{-B \pm [B^2 - 4AK_mC_L]^{0.5}\}/2A \tag{C2}$$

Numerical solutions for C_b together with associated fluxes and the kinetic advantages for delivery of glucose to the brush border in the form of polymers are shown for human jejunum in Table 6. The kinetic advantages are shown in graphical form as Figure 11 of the text.